

A Multi-Agent System Enables Versatile Information Extraction from the Chemical Literature

Yufan Chen¹, Ching Ting Leung¹, Bowen Yu¹, Jianwei Sun^{1,2}, Yong Huang²,
Linyan Li³, Hao Chen^{1,4}, Hanyu Gao^{1*}

¹Department of Chemical and Biological Engineering, The Hong Kong University of Science and Technology, Hong Kong SAR, China

²Department of Chemistry, The Hong Kong University of Science and Technology, Hong Kong SAR, China

³Department of Data Science, City University of Hong Kong, Hong Kong SAR, China

⁴Department of Computer Science and Engineering, The Hong Kong University of Science and Technology, Hong Kong SAR, China

*Corresponding Email: hanyugao@ust.hk

Abstract: To fully expedite AI-powered chemical research, high-quality chemical databases are the cornerstone. Automatic extraction of chemical information from the literature is essential for constructing reaction databases, but it is currently limited by the multimodality and style variability of chemical information. In this work, we developed a multimodal large language model (MLLM)-based multi-agent system for robust and automated chemical information extraction. It utilizes the MLLM's strong reasoning capability to understand the structure of diverse chemical graphics, decompose the extraction task into sub-tasks, and coordinate a set of specialized agents, each combining the capabilities of the MLLM with the precise, domain-specific strengths of dedicated tools, to solve them accurately and integrate the results into a unified output. Our system achieved an F1 score of 80.8% on a benchmark dataset of sophisticated multimodal chemical reaction graphics from the literature, surpassing the previous state-of-the-art model (F1 score of 35.6%) by a significant margin. Additionally, it demonstrated consistent improvements in key sub-tasks, including molecular image recognition, reaction image parsing, named entity recognition and text-based reaction extraction. This work is a critical step toward automated chemical information extraction into structured datasets, which will be a strong promoter of AI-driven chemical research.

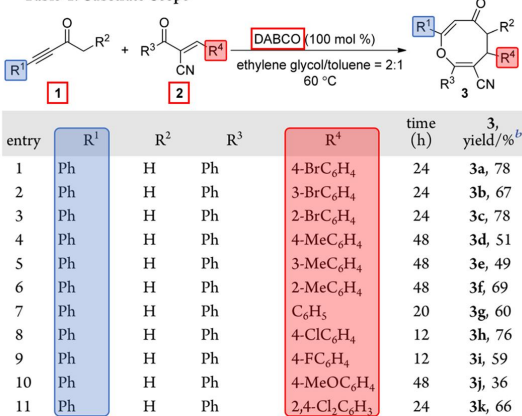
1. Main

Artificial intelligence (AI) has demonstrated significant potential in transforming chemistry research, including synthesis design, reaction prediction, and condition optimization. A crucial foundation behind these developments is the chemical databases extracted from scientific literature. Most existing databases were constructed through expert curation, and the advancement of AI research in chemistry is increasingly calling for automatic tools for data extraction (1). Nevertheless, extracting chemical information from the chemical literature has been a formidable task for computers. In chemistry publications, authors use sophisticated multimodal graphics to present rich chemistry information concisely, which is more natural for human readers but challenging for computers. **Figs. 1(a) and 1(b)** illustrate this complexity. When a set of similar reactions is performed, a template is provided as an image, and all variants are listed in an appended structure-based or text-based table, accompanied by additional text descriptions. The information is a blend of text, chemical formulas, abbreviations, identifiers, and molecular structures, and these entities are not isolated; the relationships between them need to be accurately understood to convert them into structured chemical data (2).

Research efforts have been devoted to addressing some aspects of this challenge. They mainly focused on sub-tasks such as molecular image recognition, reaction image parsing, and text-based extraction. For molecular image recognition, early studies employed rule-based algorithms and heuristic methods to translate graphical depictions into structured, machine-readable formats, such as SMILES strings (3–15). Recent advancements leveraged deep learning architectures, notably convolutional neural networks (CNNs) and transformers, significantly enhancing accuracy and robustness across various chemical notations and drawing styles (16–26). Reaction image parsing has similarly evolved, progressing from heuristic segmentation combined with image filtering to more sophisticated deep-learning approaches involving object detection and sequence-generation models, accurately identifying reactants, products, and reaction conditions within the reaction template (27–29). For text-based extraction, traditional approaches utilized rule-based parsers and keyword matching, whereas contemporary methods employ transformer-based architectures, such as fine-tuned BERT models, substantially improving the identification of chemical entities and their roles in reactions (30, 31). Recently, Fan et al. developed OpenChemIE (32), a rule-based system that integrates several previously developed tools, and attempted to extract chemical reaction information across multiple modalities, achieving some degree of success. However, its reliance on manually designed extraction rules significantly limits its scalability and adaptability to diverse chemical graphic styles and notations. With the emergence of advanced general multimodal large language models (MLLMs) (33–44), several recent works (45, 46) utilize MLLMs to identify text from chemical graphics and align them with the reaction template. However, these single-model approaches still struggle with the complex and heterogeneous nature of chemical graphics, especially due to the variability in human design thinking behind their creation, which introduces stylistic diversity that challenges automated interpretation.

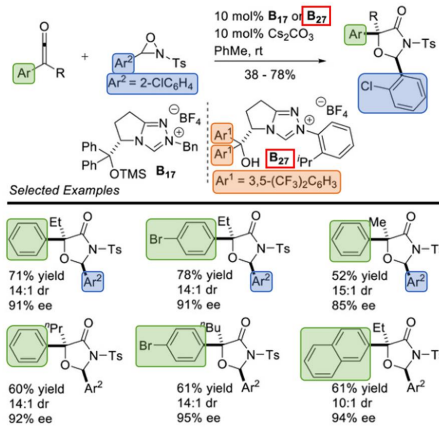
a **Image**
Text Table
Text

Table 1. Substrate Scope^a



^aReactions were performed using **1a** (0.5 mmol), **2a** (0.75 mmol), DABCO (0.5 mmol) in 3 mL of solvent (EG/Toluene = 2:1) at 60 °C. ^bIsolated yields. EG = ethylene glycol.

b



In 2010, an enantioselective formal [3+2] cycloaddition of NHC-bound azolium enolates and oxaziridines was described by Ye and co-workers. Aryl(alkyl)-disubstituted ketenes were used as precursors of azolium enolates. A bifunctional NHC precatalyst **B27** bearing a free hydroxyl group was employed.

c

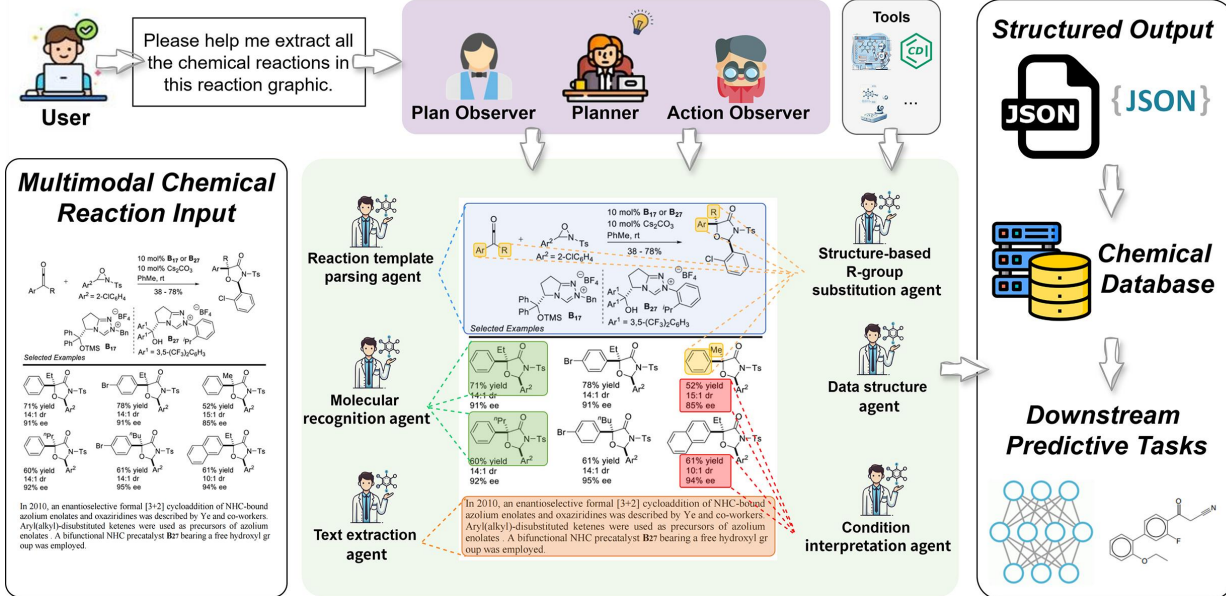


Fig. 1. Illustration of key challenges and proposed ChemEAGLE for chemical information extraction. **a,b**, Examples of chemical reaction graphics from the literature highlight the challenge of extracting information spread across images, tables, and text describing conditions and reagents. This complexity requires systems that can integrate diverse and multimodal data types. **c**, Schematic of ChemEAGLE: a planner agent coordinates specialized agents to extract information from images, tables, and text, which is then integrated into a structured output for chemical databases and AI applications.

To address these challenges, we propose a fundamentally different solution rooted in hierarchical task decomposition and multi-agent collaboration (47–55). Our core hypothesis is that, employing a central MLLM to dynamically break the extraction task into smaller, specific sub-tasks and coordinate specialized agents and tools for each, enables more accurate and flexible extraction of chemical information from stylistically diverse graphics. We developed ChemEAGLE (Chemical information Extraction by AGentic LanguagE models), a multi-agent system designed specifically for this purpose. The system is schematically presented in **Fig. 1(c)**.

In this system, a central Planner agent interprets the extraction task and plans an extraction workflow. The Planner then assigns individual specialized agents to perform sub-tasks in the workflow. The agents utilize various extraction tools to handle different sub-tasks and summarize the results into structured chemical data. The Plan observer agent evaluates the workflow proposed by the Planner, providing feedback to refine task decomposition and agent selection. The Action observer agent monitors each step of execution, catching tool failures or mismatches between intermediate outputs and the extraction plan, and prompts corrective actions when necessary. The specialized agents are also based on MLLMs, taking advantage of their excellent reasoning and analytical capabilities. We demonstrated that our system could be used to process highly sophisticated graphics from chemical publications, significantly exceeding the capability of existing models with an F1 score of 80.8% compared to 35.6% from the previous state-of-the-art model. Our system also performed consistently better on existing benchmark datasets for specific tasks, including molecular image recognition, reaction image parsing, named entity recognition and text-based reaction extraction. These results represent a significant step toward automating the extraction of chemical information to construct large-scale chemical databases and power AI research in chemistry.

2. Results

2.1 Workflow of ChemEAGLE

To effectively address the complexity and heterogeneity of chemical data embedded in modern scientific literature, ChemEAGLE employs a flexible multi-agent workflow. This design enables the system to adaptively parse, align, and integrate chemical information distributed across images, tables, and textual annotations, regardless of graphic style or modality. We illustrate an example extraction workflow for a multimodal reaction graphic containing a variant structure-based table in **Fig. 2**. ChemEAGLE first utilizes the Planner agent to analyze the input and plan the extraction steps and agents. The Reaction template parsing agent is first called to convert the reaction template into SMILES strings with R-group formulas by detecting components with RxnImgParser and Image2Graph, and corrects OCR errors to update R-group placeholders. The Molecular recognition agent locates and segments molecules using MolDetector, detects and assigns molecular coreferences, then processes each molecule with Image2Graph and Graph2SMILES to generate SMILES for product variants. The Structure-based R-group substitution agent extracts detailed R-group fragments from the product variant structure table and reconstructs reactant SMILES using the SMILESReconstructor. The Condition interpretation agent extracts and associates reaction conditions with the corresponding reaction instances, while the Text extraction agent captures and aligns additional details from the text. Finally, the Data structure agent integrates all information into a unified JSON record, ensuring each variant of the reaction is fully specified for downstream use. This multi-agent workflow enables ChemEAGLE to accurately fuse visual, tabular, and textual information, resolve cross-modal R-group substitution and coreferences, and adapt dynamically to diverse input formats. Further implementation details of the tools, agents and more extraction plans with Text-based R-group substitution agent are provided in the Method section and Supplementary Information.

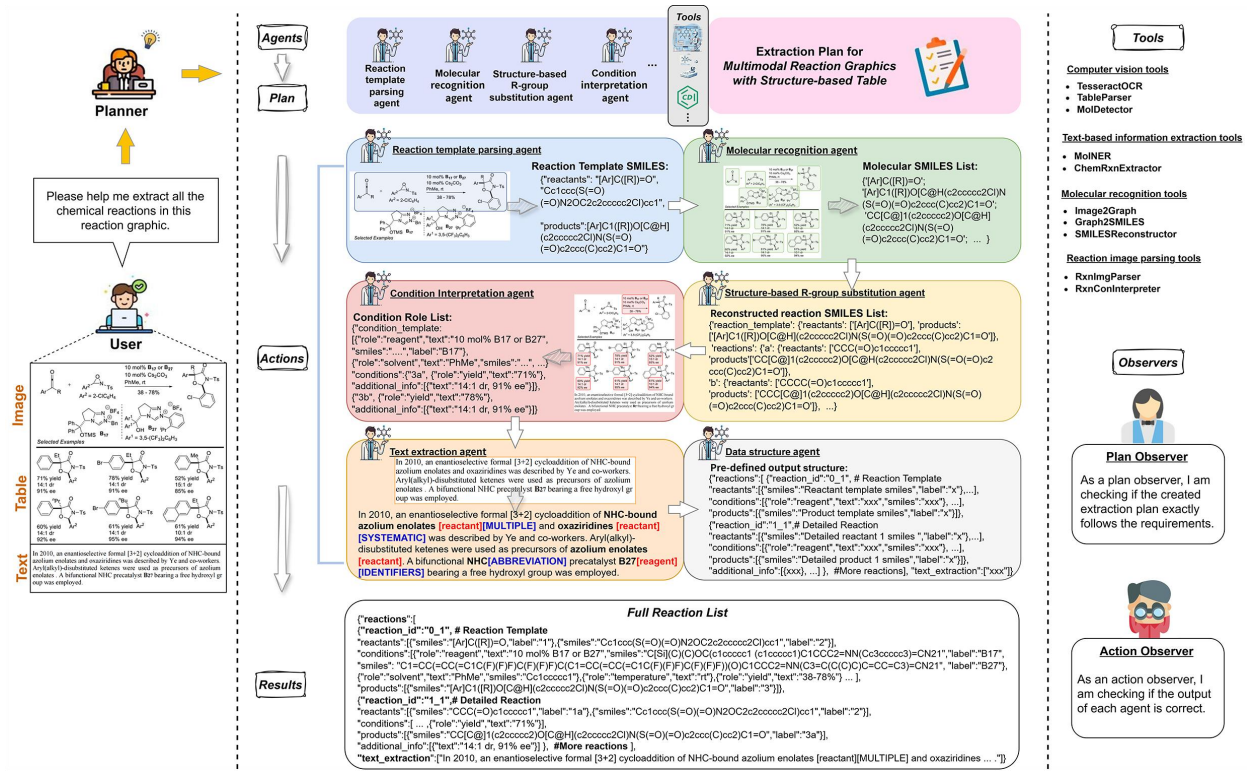


Fig. 2. Workflow demonstration of ChemEAGLE's multi-agent system for multimodal reaction graphics with structure-based tables. The user inputs sophisticated chemical reaction graphics consisting of template image, structure-based tables, and text descriptions. ChemEAGLE's Planner agent first formulates an extraction plan, sequentially assigning tasks to specialized agents: Reaction template parsing agent, Molecular recognition agent, Structure-based R-group substitution agent, Condition interpretation agent, Text extraction agent, and Data structure agent. Each agent employs computational tools and MLLM-based reasoning to parse, interpret, and reconstruct complete reaction details, effectively integrating multimodal data into a structured chemical reaction dataset. Observers ensure each agent's actions align precisely with predefined extraction requirements, further validating extraction accuracy.

2.2 Chemical information extraction from sophisticated chemical reaction graphics

2.2.1 Benchmark construction and composition

To enable rigorous evaluation of our approach and foster future research, we constructed the largest and most diverse benchmark on chemical information extraction from sophisticated multimodal chemical reaction graphics. This resource serves not only as a challenging benchmark for our method, but also as a valuable foundation for the broader community. Specifically, we first curated a dataset of 122 multimodal reaction graphics from a comprehensive organic chemistry review paper on N-heterocyclic carbene (NHC) catalysis (56) as well as 10 recent ACS journal articles, manually annotating 616 reactions with precise molecular structures, explicit reaction conditions, and metadata. Annotation was performed independently by two PhD students and reconciled by consensus after cross-checking. Additionally, we incorporated and refined a prior dataset of 78 sophisticated reaction graphics with 504 reactions in 48 recent ACS journal articles (32), further increasing the diversity and comprehensiveness of the benchmark. The benchmark includes total 200 reaction graphics with

1120 reactions and captures diverse graphical styles across modalities, including reaction graphics accompanied by (i) text-based tables with different R-group sets, (ii) text-based tables with only alternative condition, and (iii) variant structure-based tables with fully drawn molecules, supplemented by related footnotes, text descriptions or additional R-group formulas.

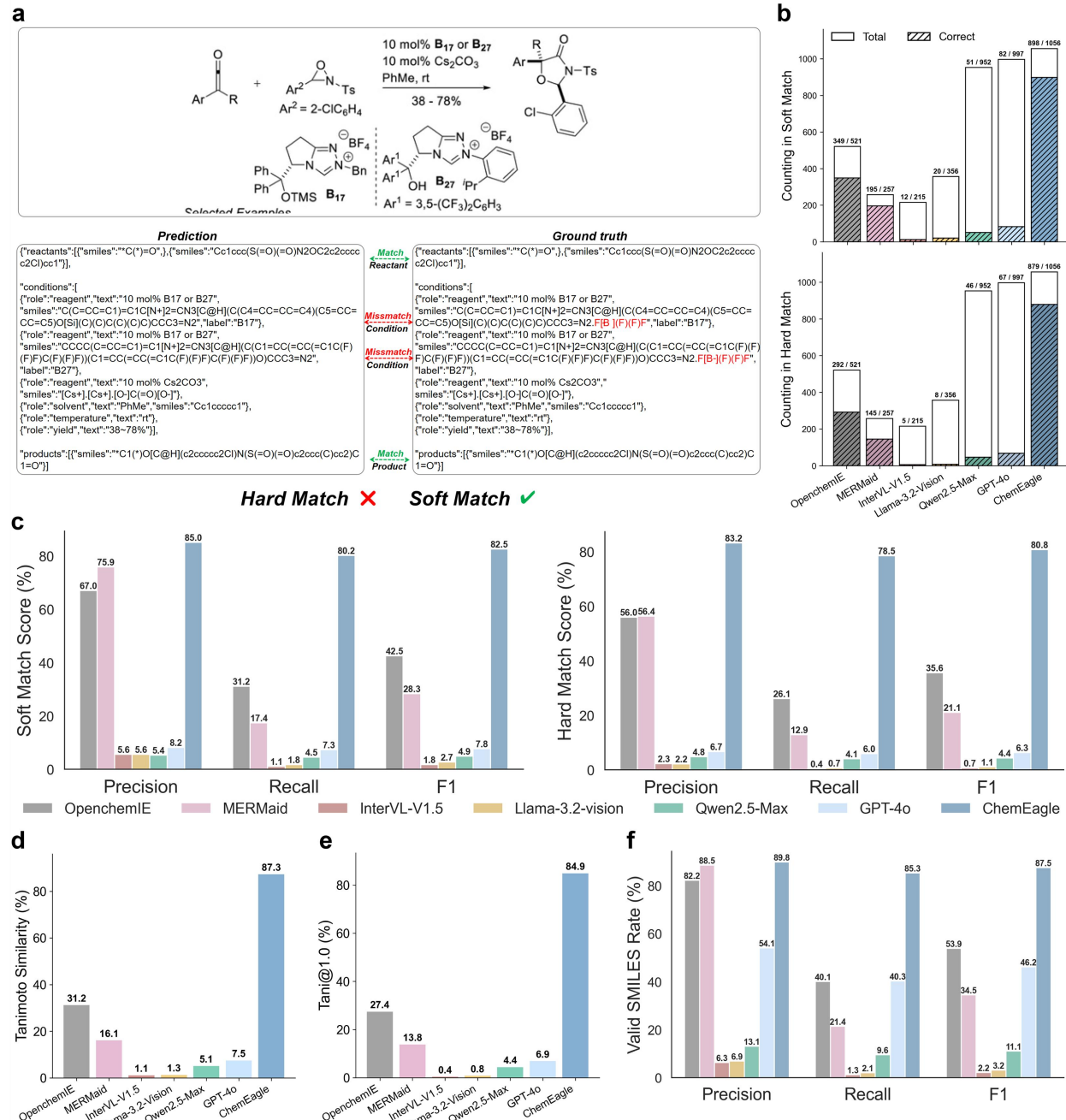


Fig. 3. Comprehensive evaluation of ChemEAGLE's multimodal chemical reaction extraction capability. **a**, Main evaluation metrics illustration. Hard match requires all the reactants, conditions, and products to be matched. Soft match only considers SMILES of reactants and products. **b**, Comparison of extraction completeness under soft match and hard match criteria, highlighting ChemEAGLE's significantly superior number of correct extractions and total prediction made compared to existing multimodal frameworks and general MLLMs. **c**,

Precision, recall, and F1-score analysis under hard-match and soft-match. **d**, Comparison of Tanimoto similarity. **e**, Comparison of Tanimoto@1.0. **f**, Comparison of valid SMILES rate, reporting precision, recall, and F1 score for the fraction of chemically valid SMILES among predictions.

2.2.2 Evaluation metrics and criteria

To assess ChemEAGLE’s ability to extract chemical information across modalities, we evaluated its performance on full reaction graphics containing images, text, and tables. The task is to extract a set of structured reactions, where each reaction consists of reactants and products (represented as SMILES) and detailed reaction conditions (including reagents, solvents, temperature, time, yield, and condition molecules as SMILES). We used two main evaluation criteria: soft-match, which requires all reactant and product SMILES to exactly match the ground truth, and hard-match, which further requires the reaction conditions to match as well (see **Fig. 3(a)**). Precision, recall, and F1 scores were calculated under both criteria. In addition, we report the widely adopted Tanimoto similarity and Tani@1.0 metrics. We also evaluated the valid SMILES rate, defined as the proportion of predicted SMILES strings that can be successfully parsed as valid molecules. We report precision, recall, and F1 scores.

2.2.3 Performance analysis and baseline comparison

We evaluated ChemEAGLE on our new benchmark dataset under both soft- and hard-match criteria, comparing it against leading systems including OpenChemIE (32), MERMAid (45), and advanced general MLLMs (57–60) (InterVL-V1.5, Llama-3.2-Vision, Qwen2.5-Max, and GPT-4o) in **Figs. 3(b)** and **3(c)**. Under the soft-match criterion, ChemEAGLE achieved the highest performance, correctly extracting 898 out of 1056 total predictions, with a precision of 85.0%, recall of 80.2%, and an F1 score of 82.5%. OpenChemIE, the best-performing baseline, achieved a lower F1 score (42.5%), limited by its rigid and elementary rule-based design and sensitivity to image and table variations. MERMAid, despite high precision (75.9%), showed low recall (17.4%) and an F1 score of 28.3%, primarily due to its reliance on a single parsing model and lack of explicit handling of R-group substitutions. General MLLMs performed substantially worse, with F1 scores below 10%. Although the top MLLMs (e.g., GPT-4o) generated many predictions, the vast majority were incorrect, reflecting a lack of domain-specific chemical structure reasoning.

Under the more rigorous hard-match criterion, which requires exact matches for reaction conditions in addition to reactants and products, ChemEAGLE maintained strong performance, correctly extracting 879 out of 1056 total predictions (80.8% F1). In contrast, OpenChemIE’s F1 score dropped sharply to 35.6% (292 correct predictions), showing the limitations of its rule-based approach for accurately parsing complex reaction conditions from tables and template images. MERMAid’s performance also declined significantly (21.1% F1). General MLLMs still performed poorly: Llama-3.2-Vision and InterVL-V1.5 achieved F1 scores of only 1.1% and 0.7%, respectively, while Qwen2.5-Max and GPT-4o achieved slightly higher scores. These results underscored the critical need for specialized chemical structure reasoning or extraction modules for accurate chemical information extraction.

The results of Tanimoto similarity and Tani@1.0 analysis (see **Figs. 3(d)** and **3(e)**) further highlight ChemEAGLE’s advantage over both rule-based and general MLLM baselines. In cases where ChemEAGLE fails to generate exact ground-truth SMILES, the predicted molecules are

substantially more similar to the references than those produced by competing approaches. This is reflected in higher overall average similarity scores, indicating that ChemEAGLE’s errors tend to be minor, such as misplaced or misassigned substituents, rather than the severe or random mistakes common in other systems. To further illustrate the robustness of our approach, we analyzed Tani@1.0 performance specifically on molecules containing challenging features such as abbreviations and chiral centers (see **Table S1**). ChemEAGLE’s accuracy on these critical subsets was only modestly reduced relative to other methods, demonstrating the ChemEAGLE’s resilience and robustness in capturing chemically salient structural information. Notably, abbreviations and stereochemistry often govern key physical or biological properties, and accurate representation of these elements is essential for reliable downstream applications. The Valid SMILES rate (see **Fig. 3(f)**) indicate nearly all predicted SMILES of ChemEAGLE are valid, making any necessary manual corrections fast and efficient. These results confirm that ChemEAGLE delivers both high accuracy and chemically plausible outputs, ensuring robust and scalable extraction across complex datasets.

2.2.4 Case studies on challenging chemical reaction graphics

To further demonstrate the practical strengths and differences between ChemEAGLE and leading baseline systems, we conducted detailed case studies on challenging chemical reaction graphics from the benchmark dataset. **Fig. 4** gives a concrete illustration of these contrasts. In the first example (see **Fig. 4(a)**), the reaction graphic presents a reaction template with R-group formulas “Ar₂ = 2-C1C6H4” and “Ar₁ = 3,5-(CF₃)₂C₆H₃”, a product variant table and footnotes specifying the base and conditions. For visualization and fair comparison, we use RDKit to generate molecular structure from the SMILES outputs produced by each extraction method. ChemEAGLE generates all seven variants with accurate reactants, products, R-group substitutions (see **Fig. 4(b)**), and reaction conditions (see **Fig. S2**). This is enabled by the collaboration between specialized agents: the Reaction template parsing and Molecular recognition agents recognize the reaction template and all the product variants in the form of SMILES; the Structure-based R-group substitution agent match the product template to the product variants and accurately determine R-group fragments and substitute them into reactant scaffolds; and the condition interpretation agent parses all annotations of experimental conditions. GPT-4o demonstrates strong general vision-language capabilities and can enumerate the template and five out of six variants, but the output remains unusable: R-groups are misplaced, base equivalents are omitted, and all generated SMILES are chemically invalid or incorrect (see **Fig. 4(c)**), although the conditions are sometimes correct (see **Fig. S3**). OpenChemIE extracts only the reaction template (see **Fig. 4(d)**). Its molecule recognition model generates SMILES for the scaffold but cannot incorporate the textual R-group formulas into the molecular graph, resulting in SMILES that lacks the correct substituents. The rule-based reconstructor relies on explicit atom labels to match templates with product variants. As these labels are absent, no reaction variants are generated. **Fig. 4(e)** presents additional representative examples comparing these methods across a range of complex multimodal reaction graphics. Each system’s predicted and reference outputs are summarized, spanning diverse graphical layouts and annotation styles. These results further confirm that ChemEAGLE consistently delivers the highest accuracy, robustly handling complicated R-group mappings, variant assignments, and condition extraction.

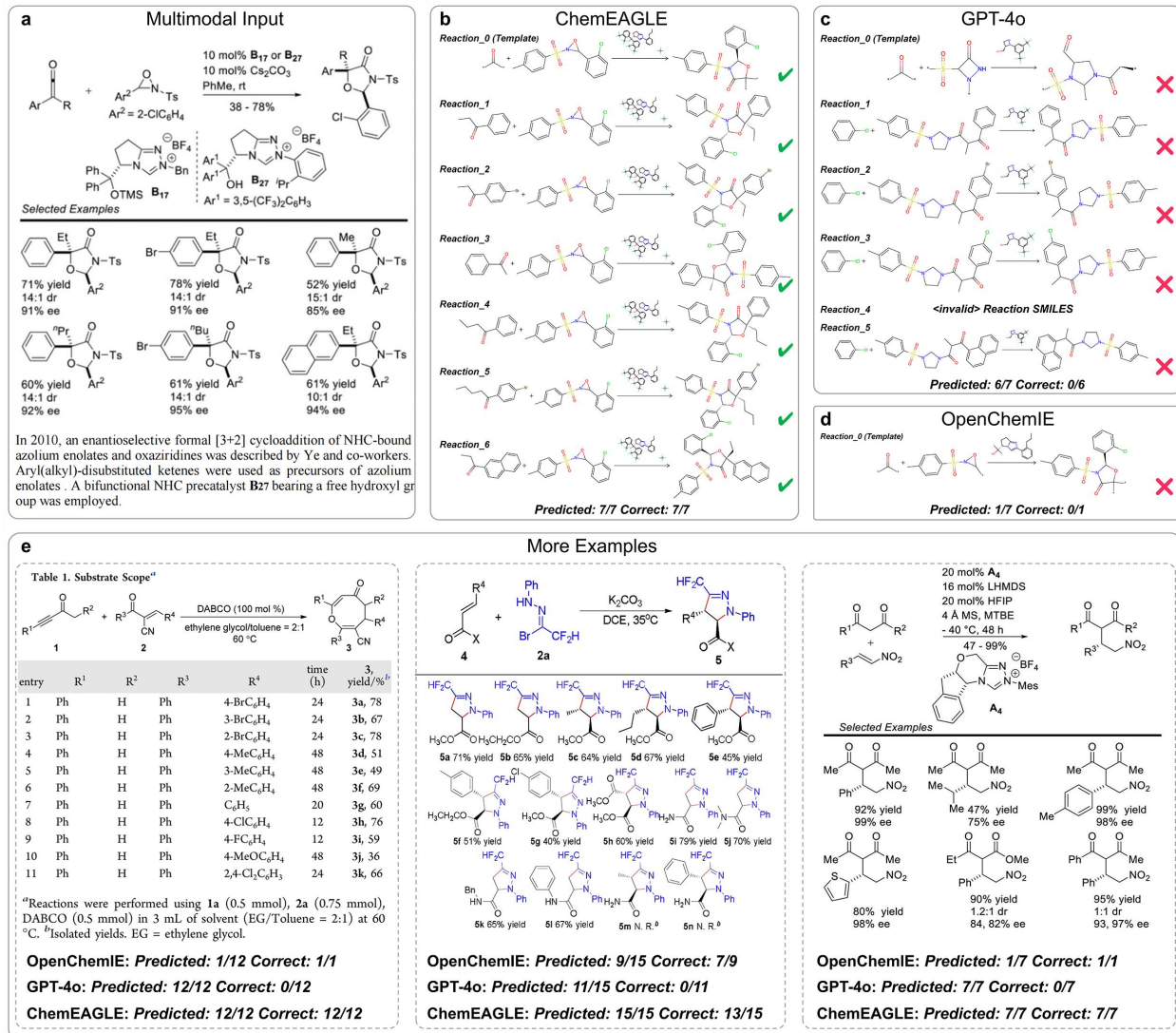


Fig. 4. Comparative visualization on some challenging multimodal reaction graphics. We show some comparative visualization of three best approaches. **a**, A challenging multimodal reaction graphic input. **b**, ChemEAGLE’s structure output. ChemEAGLE fuses R-group formulas and regenerates all seven correct reaction SMILES and conditions. Full JSON output is in **Fig. S2**. **c**, GPT-4o’s structure output. GPT-4o lists the template and five of the six variants but yields chemically incorrect or invalid SMILES. Full JSON output is in **Fig. S3**. **d**, OpenChemIE’s structure output. OpenChemIE extracts only the template SMILES without R-group substitutions and omits all reaction variants with conditions. **e**, More representative examples on diverse multimodal reaction graphics. Each system’s predicted and correct outputs are summarized.

Overall, ChemEAGLE exhibits clear and significant performance advantages under both evaluation criteria, underscoring the effectiveness and necessity of its multi-agent architecture. Within this framework, each agent tightly integrates specialized computational extraction tools with MLLM-based reasoning capabilities, while effective collaboration among agents enables precise parsing and integration of chemical information across image, text, and table. This architecture allows ChemEAGLE to accurately resolve and integrate multimodal chemical

reaction information comprehensively, effectively overcoming critical limitations of previous rule-based methods, single-modal workflows, and general MLLMs.

2.3 Performance on single-modal chemical information extraction sub-tasks

To better understand ChemEAGLE’s capabilities and potential bottlenecks, we evaluated the performance of its individual agents on critical single-modal chemical information extraction tasks. ChemEAGLE’s flexible workflow design can dynamically adapt its plan of agent assignment to match the modality and style of the input, automatically selecting the minimal set of specialized agents required for each sub-task. This generality allows ChemEAGLE to support a broad spectrum of chemical information extraction across the varied formats found in chemical literature. Consequently, it enables direct and fair benchmarking of each extraction sub-tasks, including molecular image recognition, reaction image parsing, named entity recognition, and text-based reaction extraction, on their respective standard benchmark. Detailed extraction plans for these sub-tasks can be found in the Supplementary Note 2.

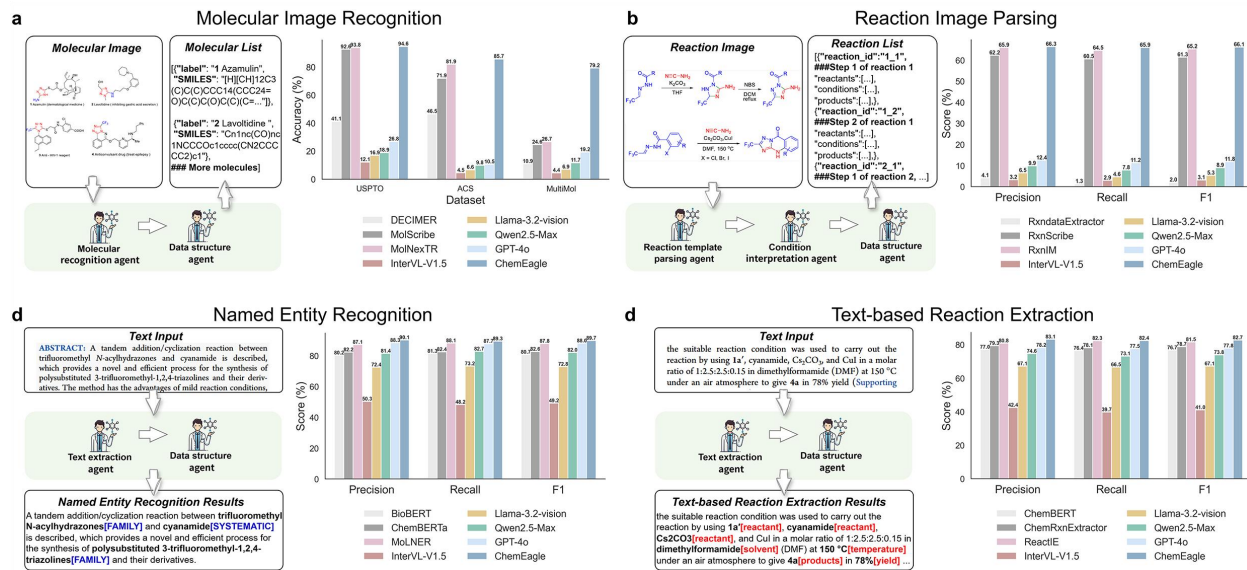


Fig. 5. Workflow and performance evaluation of ChemEAGLE on critical chemical information extraction sub-tasks. **a**, Molecular image recognition: ChemEAGLE integrates domain tools and MLLM correction, outperforming baselines on USPTO, ACS, and MultiMol. **b**, Reaction image parsing: ChemEAGLE combines parsing and condition agents for higher accuracy in extracting reactants, products, and conditions from complex schemes. **c**, Named entity recognition: The text extraction agent with MolNER and MLLM correction surpasses specialized and general models in identifying chemical entities. **d**, Text-based reaction extraction: ChemEAGLE’s agent with ChemRxnExtractor and MLLM correction achieves top performance in mapping text to structured reaction data. All tasks use the data structure agent for flexible output formatting.

2.3.1 Molecular image recognition

Molecular image recognition converts molecular images into machine-readable formats, such as SMILES strings. The right panel of **Fig. 5(a)** shows the extraction plan of ChemEAGLE for this task, which only calls the Molecular recognition agent and the Data structure agent. We benchmarked ChemEAGLE and baseline models on three datasets: USPTO (5,719 images) (61), ACS (331 images), and MultiMol (300 images with 1,610 molecules from crowded scope tables).

MultiMol, in particular, was designed to mimic the dense, multi-molecule layouts frequently found in chemical literature. As shown in **Table S2**, ChemEAGLE consistently delivers the highest rate of valid SMILES predictions on MultiMol, demonstrating much greater reliability than both specialized tools and general MLLMs. The left panel of **Fig. 5(a)** presents the exact match accuracy comparison on three datasets. ChemEAGLE achieved 94.6% on USPTO, 85.7% on ACS, and 81.5% on MultiMol, outperforming MolNexTR, MolScribe (24), DECIMER (18). Notably, on the challenging MultiMol dataset, ChemEAGLE maintains robust performance, while specialized tools initially designed for single-molecule images drop sharply to below 27%. This advantage is further supported by molecular similarity analysis in **Table S3**, which shows that ChemEAGLE produces much more chemically faithful structures than any baseline. General MLLMs uniformly underperform on all three sets. GPT-4o, the strongest of these, manages only 26.8%, 10.5%, and 19.2% on USPTO, ACS, and MultiMol, respectively.

2.3.2 Reaction image parsing

Reaction image recognition refers to the task of automatically extracting structured chemical reaction information from graphical reaction schemes. As illustrated in the right of **Fig. 5(b)**, when the input provided to ChemEAGLE is solely a reaction scheme image, the planner agent assesses the scope and complexity of the sub-task and accordingly assigns it to the Reaction template parsing agent, the Condition role interpretation agent, and the Data structure agent to parse the reaction image. The benchmark dataset consists of 138 reaction images with a total of 412 annotated reactions collected from recent chemical journal articles, presenting complex and structurally diverse reaction schemes. The left panel of **Fig. 5(b)** shows that ChemEAGLE achieves the highest hard-match F1-score (66.1%), outperforming RxnIM, RxnScribe (29), RxnDataExtractor (27). ChemEAGLE also achieves the highest valid SMILES rate, Tanimoto similarity and Tani@1.0 scores among all methods (see **Tables S4, S5**). In contrast, even the strongest general MLLM achieves less than 12% hard-match F1 on this task.

2.3.3 Named entity recognition

Named entity recognition (NER) locates and classifies chemical mentions in text into seven categories: SYSTEMATIC, IDENTIFIERS, FORMULA, TRIVIAL, ABBREVIATION, FAMILY and MULTIPLE. The right panel of **Fig. 5(c)** illustrates the workflow of ChemEAGLE for this task. The Text extraction agent only utilizes the MolNER tool. We use the CHEMDNER (62) corpus, which consists of 3,000 samples containing a total of 25351 chemical mentions, as the benchmark. The left of **Fig. 5(c)** summarizes the NER results, comparing ChemEAGLE against several existing specialized chemical NER models, including BioBERT (63), ChemBERTa (64), and MolNER, and general MLLMs. ChemEAGLE achieves the highest F1-score of 89.8%. Among specialized models, MolNER achieves an F1-score of 87.6%, followed by ChemBERTa (82.8%) (64) and BioBERT (80.7%) (63). Among the general MLLMs, GPT-4o demonstrates a robust chemical entity extraction capability with an F1-score of 87.9%, surpassing all other general MLLMs and performing comparably to specialized chemical NER models.

2.3.4 Text-based reaction extraction

Text-based reaction extraction identifies reactions and their roles from scientific text. The right panel of **Fig. 5(d)** shows the agent workflow, which utilizes the Text extraction agent only to access the ChemRxnExtractor tool on the benchmark Reaction Corpus (65). This corpus includes 111 annotated chemical reactions across 33 paragraphs in scientific papers. The left panel of **Fig. 5(d)** summarizes performance. ChemEAGLE achieved the highest F1-score (82.7%), followed

by ReactIE (81.6%) (66), ChemRxnExtractor (78.7%) (1), ChemBERT (76.7%) (67), and GPT-4o (77.8%) (60). Notably, compared to image-based extraction tasks, general MLLMs like GPT-4o show much stronger results on text-based tasks, indicating their inherent advantage in language understanding. Nevertheless, ChemEAGLE’s agent-based approach ensures that it remains the top performer, even as MLLMs continue to improve in text extraction.

3. Discussion

ChemEAGLE leverages the unique strengths of specialized extraction tools and the advanced multimodal reasoning capabilities of GPT-4o, demonstrating remarkable performance in complex chemical information extraction tasks, as well as single-modal sub-tasks including molecular recognition, reaction image parsing, reaction extraction, and NER.

A key strength of ChemEAGLE lies in its multi-agent integration, which allows the flexible decomposition and distribution of complex multimodal chemical extraction tasks across specialized agents. Unlike traditional single-agent or rule-based methods, ChemEAGLE leverages coordinated agent interactions to adaptively handle diverse graphic layouts and textual presentations commonly encountered in chemical literature. Specifically, the Planner agent strategically decomposes complex extraction task into clearly defined sub-tasks, dynamically assigning specialized agents for molecular recognition, reaction template parsing, table interpretation, R-group substitution and textual analysis. Each agent independently integrates specialized extraction tools with robust MLLM-based reasoning, enabling precise, context-aware extraction within its sub-task and adaptively utilizing tool to extent outputs, correct errors or resolve ambiguities where needed. This approach also enables ChemEAGLE to consistently achieve the best results across all sub-task benchmarks. Moreover, the structured collaboration between agents ensures that information extracted from different modalities (image, text, table) can be systematically integrated and validated, significantly reducing errors and enhancing overall extraction accuracy. As demonstrated in our evaluation, this collaborative design provides exceptional flexibility and robustness, enabling ChemEAGLE to accurately handle various multimodal chemical information, ultimately leading to comprehensive, accurate, and scalable chemical information extraction suitable for large-scale AI-driven chemistry applications.

We conducted an error analysis to pinpoint where ChemEAGLE’s remaining failures arise. As shown in **Fig. 6(a)**, nearly 36% of the hard-match errors originate in the Molecular recognition agent, primarily from missed molecule boxes and molecular recognition errors (see **Fig. 6(b)**). Another 26% of errors stem from the Structure-based R-group substitution agent, mainly due to undefined attachment points for R-groups—for instance, when a generic "R-Ph" label floats above a benzene ring, the attachment position is ambiguous, breaking the Image-to-Graph-to-SMILES conversion and resulting in invalid template SMILES (see **Fig. 6(c)**), which further leads to the SMILES reconstruction error of specific reaction instances (see **Fig. 6(d)**).

Additionally, 24% of errors arise from the Text-based R-group substitution agent, where the connection site can be wrong when table cells use out-of-domain R-group names (see **Fig 6(e)**). Although the Base MLLM can reason over outputs and correct many issues, its effectiveness is fundamentally constrained by the quality of initial tool predictions. Addressing these challenges will require improvements in core extraction tools, more robust name-to-SMILES and image-to-graph modules, and further domain-specific fine-tuning of base MLLMs. The model is made

publicly available on a user-friendly interface, and its performance can be further improved based on collected user annotations and feedback.

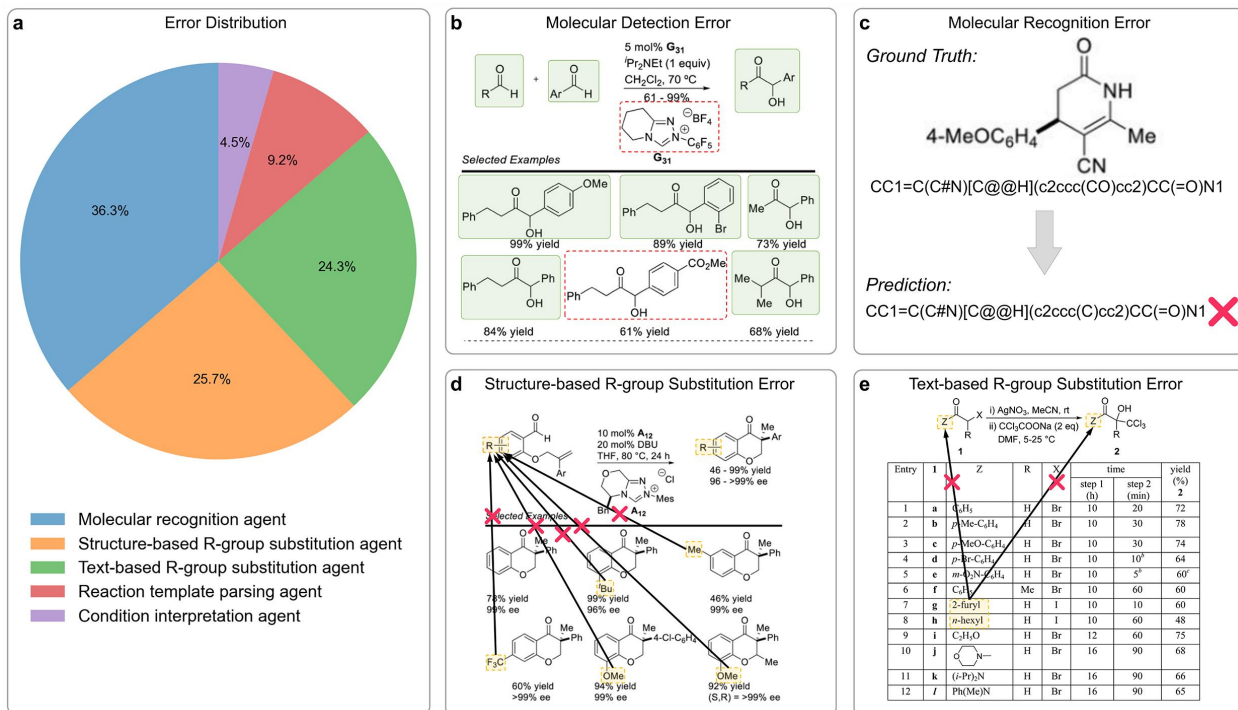


Fig. 6. Error analysis of ChemEAGLE's extraction. **a**, Hard-match error distribution across agents. **(b-e)** represents the four most common errors: **b**, Missing two small molecules during molecular detection and reaction template parsing; **c**, Molecular recognition error for a R-group abbreviation; **d**, Structure-table R-group substitution failed caused by ambiguous R-group placement; **e**, Text-table R-group substitution failed when some out-domain R-group names appear in cells.

In conclusion, our work highlights the significant potential of multi-agent multimodal frameworks for automating chemical reaction information extraction, paving the way for more comprehensive, accurate, and scalable chemical knowledge curation. By addressing the identified limitations, continuously refining extraction tools, and expanding system capabilities, ChemEAGLE holds promise as a versatile and powerful assistant for chemical researchers, driving forward data-driven advancements in chemistry and related fields.

4. Methods

4.1 Base MLLM

Due to the inherently multimodal nature of chemical information extraction tasks, which require simultaneous analysis of text, tables, and images, it is crucial to select an MLLM with robust visual reasoning and multimodal understanding. We therefore selected GPT-4o, currently one of the OpenAI's most advanced MLLM, as our base model. GPT-4o effectively integrates textual, tabular, and visual information, providing the necessary multimodal reasoning capacity required by ChemEAGLE. For all experiments, we utilized GPT-4o with a temperature setting of 0.1 to ensure precise and consistent reasoning performance.

4.2 Tools

The tools used can be classified into computer vision tools, text-based chemical information extraction tools, molecular image recognition tools, and reaction image parsing tools. The tools can be further expanded and improved as needed according to task requirements and tool availability.

4.2.1 Computer vision tools

TesseractOCR. TesseractOCR (68) is an open source optical character recognition (OCR) tool optimized for extracting textual information from graphics. In ChemEAGLE, TesseractOCR is employed by the Base GPT-4o to extract the text embedded in chemical graphics, facilitating the extraction of chemical names, reaction conditions, and experimental notes embedded within chemical graphics. Given the specialized terminology and symbol-heavy nature of chemical graphics, its performance is enhanced through customized preprocessing techniques, including adaptive thresholding, noise reduction, and character segmentation. Additionally, post-processing steps such as context-aware spelling correction further refine the extracted text, ensuring that critical reaction details are preserved with high accuracy. This process establishes a reliable foundation for subsequent extraction, ensuring that extracted reaction details can be accurately analyzed and integrated into structured datasets.

TableParser. TableParser is a specialized tool designed to accurately extract and reconstruct text-based data from reaction tables. Reaction tables often encapsulate critical experimental details such as reaction conditions, yields, reagents and different R-group sets. It employs a multi-stage deep learning approach to first detect table boundaries using a CNN and then segment the table into individual rows and cells. Each cell is subsequently processed with the TesseractOCR to reliably capture the contained text. This structured, machine-readable representation of tables enables seamless integration with other components of the reaction information extraction pipeline, ensuring that essential tabular data is effectively utilized in subsequent extraction.

MolDetector. In ChemEAGLE, we develop the MolDetector, a molecule detection model formulated with sequence generation as the molecular object detection tool. Inspired by the Pix2Seq (69) model designed for object detection, MolDetector identifies molecular sub-images by predicting their bounding boxes as a sequence. Given a graphic, a molecule entity whose bounding box has top-left coordinates (x1, y1) and bottom-right coordinates (x2, y2) is represented as five discrete tokens, [[x1],[y1],[x2],[y2],[mol]], where [Mol] is a special token that indicates the detection of a molecule. MolDetector sequentially generates all the molecule entities within the graphic. MolDetector is implemented as an encoder-decoder architecture. The graphic is encoded using a CNN to obtain hidden representations. Then, the decoder is a Transformer that generates the output sequence to obtain the final molecular object detection result. More detailed implementation details of MolDetector can be found in Supplementary Note 3.

4.2.2 Text-based chemical information extraction tools

MolNER. In ChemEAGLE, we develop MolNER, a specialized model trained to recognize and classify chemical entities in scientific literature. To ensure high accuracy and domain relevance, MolNER is trained on the publicly available CHEMDNER corpus, which consists of PubMed abstracts with expert-annotated chemical entity mentions. The model follows a sequence tagging approach using the BIO (Beginning, Inside, Outside) format, which enables precise token-level

classification of chemical names. To enhance performance and domain-specific understanding, MolNER is fine-tuned on a BioBERT-Large pretrained on biomedical literature, leveraging contextual embeddings that capture the nuances of chemical terminology. This approach improves the model's ability to disambiguate entity mentions and recognize diverse naming conventions that ensure a reliable and scalable extraction of chemical entities from text. More detailed implementation details can be found in Supplementary Note 4.

ChemRxnExtractor. ChemEAGLE incorporates ChemRxnExtractor, a deep learning-based model previously developed for text-based reaction extraction (1). ChemRxnExtractor follows a two-stage structured prediction framework. The first stage employs a sequence tagging model to identify reaction product mentions, while the second stage applies a relation extraction model to assign reaction roles (e.g., reactants, catalysts, solvents) to each identified product. This hierarchical approach ensures a structured and interpretable representation of reaction data. ChemRxnExtractor is trained on a large-scale expert-annotated chemical literature dataset. To enhance generalization and robustness, the model is fine-tuned on a domain-adapted transformer encoder, which is pretrained on a large corpus of chemical texts. Additionally, an adaptive pretraining strategy is employed, leveraging unlabeled reaction-rich texts to improve model performance on low-resource scenarios. By integrating context-aware chemical entity resolution and syntactic parsing, ChemRxnExtractor achieves high precision in identifying and linking reaction components across diverse writing styles. More detailed implementation details of ChemRxnExtractor can be found in Supplementary Note 5.

4.2.3 Molecular recognition tools

Image2Graph. Image2Graph is a molecular image recognition tool designed to convert molecular images into detailed graph representations that include sets of atom symbols, atom coordinates and bonds. In ChemEAGLE, Image2Graph is developed based on our previously developed MolNexTR (70). It leverages a hybrid vision-based architecture that combines CNNs and Vision Transformers to extract rich visual features from molecular images. This feature representation is then processed by a transformer-based graph reconstruction module, which predicts atom nodes and bond edges, effectively converting visual representation into structured chemical graphs. By sequentially parsing visual cues and inferring the underlying molecular connectivity, the tool effectively bridges the gap between pixel-level representations and structured chemical graphs. This approach is robust to diverse drawing styles and image noise, ensuring that even complex chemical structures are accurately captured for subsequent extraction. More detailed implementation details of Image2Graph can be found in Supplementary Note 6.

Graph2SMILES. Graph2SMILES is a rule-based method that utilizes RDKit for SMILES generation from graphs. Graph2SMILES takes as input the molecular graphs obtained from Image2Graph, which contain atom nodes and bond edges extracted from chemical structures. The tool applies predefined chemical rules alongside RDKit's molecular structure processing algorithms to generate accurate SMILES representations. This rule-based approach ensures high stability and interpretability when processing well-defined molecular graph data, allowing for precise conversion across various molecular structures. One of the major challenges in chemical information extraction is that R-groups often serve as placeholders in reaction templates, with their detailed identities provided separately in tables or annotations. By separating Image2Graph and Graph2SMILES, ChemEAGLE can first extract generic graph representations and subsequently resolve R-groups, whether they appear in tables or directly in graphics. More detailed implementation details of Graph2SMILES can be found in Supplementary Note 7.

SMILESReconstructor. SMILESReconstructor is an RDKit-based tool designed to address another fundamental challenge in chemical information extraction: the incomplete representation of reactant structures in reaction graphics. In many cases, reaction graphics depict multiple product variant structures with distinct R-group substitutions, while omitting explicit illustrations of the corresponding reactant variants. This lack of direct structural representation can hinder accurate reaction reconstruction, requiring an automated approach to infer the missing reactant structures from available product information. SMILESReconstructor overcomes this challenge by first extracting R-group SMILES fragments from the product variant structures. It then intelligently maps these fragments onto a predefined reactant template, reconstructing the full reactant structures with high fidelity. This process ensures that all chemically relevant modifications in the product variants are accurately reflected in the corresponding reactants. Leveraging RDKit's substructure matching and chemical manipulation capabilities, SMILESReconstructor ensures that the integration of R-group fragments into the template maintains the correct chemical connectivity and preserves the original reaction context. The automated reconstruction minimizes the risk of manual errors and improves efficiency as well. More detailed implementation details of SMILESReconstructor can be found in Supplementary Note 8.

4.2.4 Reaction image parsing tools

RxnImgParser. RxnImgParser is a reaction image parsing tool built upon RxnIM (71), a deep learning model we previously developed for processing complex reaction images. Designed specifically for reaction templates, RxnImgParser focuses on extracting structured reaction information from image-based representations of chemical transformations. Unlike general molecule recognition tools, it is specialized in detecting and analyzing reaction templates, which depict the core transformation patterns without explicit substrate scope details. Leveraging RxnIM's integrated vision-language understanding, RxnImgParser performs both object detection and role classification within reaction templates. The tool first uses the same sequence as MolDetector to identify and segment key reaction components, such as molecular structures and text regions, detecting their precise coordinates in the image. Beyond simple localization, RxnImgParser extends this sequence to determine the reaction roles of detected components within the reaction scheme such as reactants, reagents, conditions, and products. Given that reaction templates often depict multi-step reaction cascades, RxnImgParser is capable of resolving molecule roles across different steps, recognizing cases where a molecular entity simultaneously acts as the product of one reaction and the reactant of the next. The implementation detail can be found in Supplementary Note 9.

RxnConInterpreter. RxnConInterpreter is also built upon RxnIM (71) but only focuses on the textual information within reaction condition regions to interpret reaction condition. By utilizing the same MLLM backbone and adding different task prompt, RxnConInterpreter performs integrated optical character recognition and contextual analysis to extract and interpret the text embedded in these regions. It not only extracts the text but also classifies each element into predefined condition roles such as reagent, solvent, time, yield, and temperature, ensuring that the nuanced details of the reaction conditions are accurately captured. This targeted interpretation of condition information complements the overall extraction process. The implementation detail can be found in Supplementary Note 9.

4.3 Agents

In this section, we present the various agents in ChemEAGLE, illustrating their extraction processes and the combination of tools they utilize. Each agent is designed to handle a different sub-task to ensure the accuracy of the final extraction result. All agents except the Text-based R-group substitution agent use **Fig. 1(b)** as the example input. The Text-based R-group substitution agent use **Fig. 1(a)** as the example input. Detailed implementation information for all agents is provided in the Supplementary Information.

4.3.1 Planner

The Planner agent serves as the central coordinator of the ChemEAGLE framework. Upon receiving a multimodal chemical input, the Planner agent analyzes the overall structure and content, automatically identifying the presence of reaction templates, product variants, text tables, and descriptive paragraphs. Based on this assessment, the Planner dynamically decomposes the extraction task into an ordered sequence of sub-tasks, and allocates these to the appropriate specialized agents. The Planner thus ensures that each modality is processed by the most suitable tools and that information flows seamlessly between agents, enabling ChemEAGLE to flexibly adapt its workflow to diverse and complex input formats.

4.3.2 Plan observer

The Plan observer agent is responsible for quality control at the planning stage. After the Planner agent generates an extraction plan, the Plan observer reviews the sequence and logic of assigned sub-tasks, checking for omissions, redundancies, or inconsistencies. By verifying that the extraction workflow covers all relevant input elements and follows domain best practices, the Plan observer minimizes errors in the initial design, ensuring that the workflow is both comprehensive and efficient before any extraction is executed.

4.3.3 Action observer

The Action observer agent performs stepwise monitoring and validation throughout the extraction process. After each specialized agent completes its assigned task, the Action observer evaluates the output for correctness, completeness, and logical consistency such as verifying that recognized molecules match the detected regions, or that SMILES strings have valid syntax. If discrepancies or errors are detected, the Action observer can prompt re-execution or correction by the relevant agent. This ongoing supervision guarantees high-quality results at every stage and helps maintain end-to-end reliability across complex extraction workflows.

4.3.4 Reaction template parsing agent

The Reaction template parsing agent is designed to automatically detect and interpret reaction template images. Its goal is to accurately identify all molecular structures, relevant R-group substitutions, and other reaction elements in order to construct a reliable reaction template. The agent first applies RxnImgParser to locate and segment distinct molecular regions within the template image, assigning bounding boxes that distinguish reactants, products, or other relevant components. Once these bounding boxes are identified, it invokes Image2Graph to translate each molecular structure into a graph representation, capturing atoms, bonds, and overall connectivity. Next, it analyzes R-group annotations or equations (e.g., "Ar₂ = 2-ClC₆H₄") to replace placeholders such as "[Ar2]" in the atom set in graph information with explicit substituents such as "[2-ClC6H4]" and correct OCR error in the Image2Graph tool output. After updating the graph with these R-group substitutions, the agent calls Graph2SMILES to generate the final SMILES strings, thus creating a complete reaction template that is ready for subsequent extraction.

4.3.5 Molecular recognition agent

The Molecular recognition agent is designed to detect and interpret all molecules present within a chemical graphic, including the molecules in the reaction template and all product variants. Its objective is to accurately capture each molecule, convert its visual depiction into a detailed graph representation, incorporate any R-group substitution information extracted from the graphic, and finally generate standardized SMILES strings. Initially, the agent first calls MolDetector to scan the graphic and detect every molecule sub-images. It then detects and assigns molecular coreferences. Following this detection, it leverages Image2Graph to translate the visual depictions into graph information that encapsulates atoms, bonds, and spatial connectivity. Same as the Reaction template parsing agent, it examines the R-group annotations or equations in the graphic, identifying the equations and substitutes placeholders in the corresponding atom sets. It also corrects OCR error in the Image2Graph tool output. In this example, it corrects "iP1" to "iPr". Finally, Graph2SMILES tool is called to convert the updated graphs into precise SMILES strings, ensuring that each molecule is accurately represented for subsequent extraction.

4.3.6 Structure-based R-group substitution agent

The Structure-based R-group substitution agent is specifically designed to handle cases where reaction graphics explicitly depict multiple product variant structures in a table without directly illustrating their corresponding reactant variant structures. It calls upon SMILESReconstructor to perform substructure matching between each product variant and the product template, isolating the R-group SMILES fragments in the process. Once the R-group fragments are extracted, the agent substitutes them into the corresponding positions in the reactant template, thereby accurately reconstructing the full reactant variants. This ensures that each modified product variant is consistently and correctly linked back to its corresponding reactant structure for further extraction and downstream tasks.

4.3.7 Text-based R-group substitution agent

The Text-based R-group substitution agent is designed for scenarios in which reaction graphics are accompanied by text-based tables explicitly defining R-group substitutions. After receiving structured outputs from the Reaction template parsing agent and the Molecular recognition agent, this agent utilizes the TableParser tool to extract detailed R-group substitution data from the associated tables. It then systematically replaces initial R-group placeholder atoms in both reactant and product molecular graphs with these extracted substituents. Subsequently, the agent invokes the Graph2SMILES tool to generate comprehensive and chemically accurate SMILES representations for each reaction variant, effectively reconstructing all reactant–product combinations defined by the specific R-group substitutions provided in the corresponding table.

4.3.8 Condition interpretation agent

The Condition interpretation agent specializes in extracting and interpreting textual condition information embedded within reaction graphics. Utilizing the TesseractOCR tool and RxnConInterpreter tool, the agent accurately assigns specific condition roles, such as reagents, solvents, temperatures, time, and yields, to each extracted text segment. This categorization clarifies the chemical context of reaction conditions, facilitating their integration into structured reaction data. By utilizing the agent to systematically classifying each textual condition element, ChemEAGLE significantly enhances the interpretability of reaction schemes, enabling more comprehensive extraction.

4.3.9 Text extraction agent

The Text extraction agent is used to extract chemical reactions directly from textual descriptions associated with reaction graphics. It leverages the TesseractOCR tool to first extract the text description what is embedded in graphics, then invoke MolNER tool to perform chemical named entity recognition, accurately identifying chemical entities within the text. Subsequently, the agent applies ChemRxnExtractor to extract structured reaction details, systematically linking reactants, products, reagents, and reaction conditions described within the text. It then aligns the text information with other modalities. In **Fig. 1(b)**, B27 appears in the text description and its structure appears in the reaction template, the agent will capture the structure information in the previous agent output and put it in the text extraction results. By precisely capturing reaction information embedded in textual formats and aligning it with other modalities, ChemEAGLE complements image-based and table-based extraction, ensuring comprehensive chemical reaction data extraction across multiple modalities.

4.3.10 Data structure agent

The Data structure agent consolidates and structures outputs from previously described agents into a coherent, standardized, and machine-readable format. Rather than relying on external tools, this agent utilizes a clearly defined output schema specified within its task prompt. Its primary responsibility is to systematically organize extracted reaction components, including SMILES representations, annotated reaction conditions, and text-derived information, ensuring they are accurately aligned and validated according to the predefined structure. The output structures for the four sub-tasks are also clearly defined and can be easily modified, ensuring the flexibility of ChemEAGLE. This structured and flexible consolidation is essential for supporting the automated construction of new, large-scale chemical reaction datasets, which subsequently enables efficient and reliable downstream applications such as automated reaction prediction, retrosynthesis planning, and large-scale chemical data analysis, ultimately facilitating advanced data-driven chemical research.

4.4 Multi-agent framework

ChemEAGLE's multi-agent system is mainly built upon the AutoAgents (72) framework, a comprehensive and adaptive paradigm designed to dynamically coordinate specialized agents into a cohesive team to tackle complex tasks. This framework mimics human collaborative problem solving by decomposing tasks into two distinct phases: the Drafting Stage and the Execution Stage, each endowed with a set of functionalities that ensure precision, scalability, and adaptability. In ChemEAGLE, this framework dynamically coordinates a suite of specialized chemical information extraction agents, each designed to extract specific chemical information from different modal sources such as text, images, and tables.

In the drafting stage, the framework dynamically generates an optimal team of agents and a customized execution plan. This process begins with the Planner, an agent that dissects the task and formulates an initial agent roster and step-by-step plan. The Planner collaborates with the Plan observer, which provide feedback on both the agent composition and the execution plan. These interactions ensure that the agent team is both diverse and perfectly aligned with the task requirements. In ChemEAGLE, the system's ability to dynamically assign specialized extraction agents, ensures that each aspect of the chemical information extraction process is addressed with precision.

In transitioning to the execution stage, the framework employs an Action observer to coordinate the execution of the plan. Each specialized agent engages in a cycle of self-refinement and collaborative refinement. Self-refinement enables individual agents to internally evaluate and improve their outputs based on immediate feedback, while collaborative refinement facilitates in-depth discussions among agents to reconcile different perspectives and achieve a consensus. To support these iterative processes, the framework integrates a knowledge sharing mechanism comprising short-term memory (for immediate action details), long-term memory (to archive historical execution data), and dynamic memory (which extracts and adapts critical information for subsequent steps). In ChemEAGLE, this robust memory integration empowers agents to dynamically leverage both recent and historical insights, ensuring the extraction process remains accurate and adaptive.

By combining dynamic agent generation, iterative plan refinement, and robust memory integration, the AutoAgents framework delivers a versatile solution that not only scales to a wide range of complex tasks, but also continuously enhances its performance through coordinated inter-agent communication and feedback loops. ChemEAGLE, based on this framework, provides an effective, scalable, and reliable solution for automated multimodal chemical information extraction. This holistic approach not only simplifies the process of extracting complex chemical information from different modal sources but also enhances the consistency and accuracy of the results.

References

1. J. Guo, A. S. Ibanez-Lopez, H. Gao, V. Quach, C. W. Coley, K. F. Jensen, R. Barzilay, Automated chemical reaction extraction from scientific literature. *Journal of chemical information and modeling* 62, 2035–2045 (2021).
2. M. P. Polak, D. Morgan, Extracting accurate materials data from research papers with conversational language models and prompt engineering. *Nat Commun* 15, 1569 (2024).
3. J. R. McDaniel, J. R. Balmuth, Kekule: OCR-optical chemical (structure) recognition. *J. Chem. Inf. Comput. Sci.* 32, 373–378 (1992).
4. R. Casey, S. Boyer, P. Healey, A. Miller, B. Oudot, K. Zilles, “Optical recognition of chemical graphics” in *Proceedings of 2nd International Conference on Document Analysis and Recognition (ICDAR ’93)* (1993; <https://ieeexplore.ieee.org/document/395658>), pp. 627–631.
5. P. Ibison, M. Jacquot, F. Kam, A. Neville, R. W. Simpson, C. Tonnelier, T. Venczel, A. P. Johnson, Chemical literature data extraction: the CLiDE Project. *Journal of Chemical Information and Computer Sciences* 33, 338–344 (1993).
6. Aniko T. Valko, A. T. Valko, A. Peter Johnson, A. Peter Johnson, A. P. Johnson, CLiDE Pro: the latest generation of CLiDE, a tool for optical chemical structure recognition. *Journal of Chemical Information and Modeling* 49, 780–787 (2009).

7. I. V. Filippov, M. C. Nicklaus, Optical Structure Recognition Software To Recover Chemical Information: OSRA, An Open Source Solution. *J. Chem. Inf. Model.* 49, 740–743 (2009).
8. J. Park, G. R. Rosania, K. A. Shedden, M. Nguyen, N. Lyu, K. Saitou, Automated extraction of chemical structure information from digital raster images. *Chemistry Central Journal* 3, 4 (2009).
9. N. M. Sadawi, A. P. Sexton, V. Sorge, “Chemical structure recognition: a rule-based approach” in Document Recognition and Retrieval XIX (SPIE, 2012; <https://www.spiedigitallibrary.org/conference-proceedings-of-spie/8297/82970E/Chemical-structure-recognition-a-rule-based-approach/10.1117/12.912185.full>) vol. 8297, pp. 101–109.
10. V. Smolov, F. Zentsev, M. Rybalkin, “Imago: Open-source toolkit for 2D chemical structure image recognition” in The Twentieth Text REtrieval Conference (TREC 2011) Proceedings (2011).
11. M. Zimmermann, “Chemical structure reconstruction with chemoCR” in The Twentieth Text REtrieval Conference (TREC 2011) Proceedings (2011).
12. A. Fujiyoshi, K. Nakagawa, M. Suzuki, Robust Method of Segmentation and Recognition of Chemical Structure Images in ChemInfty. (2011).
13. L. Ratnayaka, P. S. U. De Silva, H. N. M. Wijesiri, A. M. Samaradiwakara, N. Ranpatabendi, U. Rajapaksha, E-learning based chemical information extracting tool (eChem). (2012).
14. P. Frasconi, F. Gabbrielli, M. Lippi, S. Marinai, Markov Logic Networks for Optical Chemical Structure Recognition. *J. Chem. Inf. Model.* 54, 2380–2390 (2014).
15. M. Karthikeyan, Chemical structure recognition tool (2017).
16. J. Staker, K. Marshall, R. Abel, C. M. McQuaw, Molecular Structure Extraction from Documents Using Deep Learning. *J. Chem. Inf. Model.* 59, 1017–1029 (2019).
17. M. Oldenhof, A. Arany, Y. Moreau, J. Simm, ChemGrapher: Optical Graph Recognition of Chemical Compounds by Deep Learning. *J. Chem. Inf. Model.* 60, 4506–4517 (2020).
18. K. Rajan, A. Zielesny, C. Steinbeck, DECIMER: towards deep learning for chemical image recognition. *Journal of Cheminformatics* 12, 65 (2020).
19. K. Rajan, A. Zielesny, C. Steinbeck, DECIMER 1.0: deep learning for chemical image recognition using transformers. *Journal of Cheminformatics* 13, 61 (2021).
20. I. Khokhlov, L. Krasnov, M. V. Fedorov, S. Sosnin, Image2SMILES: Transformer-Based Molecular Optical Recognition Engine. *Chemistry–Methods* 2, e202100069 (2022).
21. Z. Xu, J. Li, Z. Yang, S. Li, H. Li, SwinOCSR: end-to-end optical chemical structure recognition using a Swin Transformer. *Journal of Cheminformatics* 14, 41 (2022).

22. S. Yoo, O. Kwon, H. Lee, “Image-to-Graph Transformers for Chemical Structure Recognition” in ICASSP 2022 - 2022 IEEE International Conference on Acoustics, Speech and Signal Processing (ICASSP) (2022; <https://ieeexplore.ieee.org/document/9746088>), pp. 3393–3397.

23. Y. Xu, J. Xiao, C.-H. Chou, J. Zhang, J. Zhu, Q. Hu, H. Li, N. Han, B. Liu, S. Zhang, J. Han, Z. Zhang, S. Zhang, W. Zhang, L. Lai, J. Pei, MolMiner: You Only Look Once for Chemical Structure Recognition. *J. Chem. Inf. Model.* 62, 5321–5328 (2022).

24. Y. Qian, J. Guo, Z. Tu, Z. Li, C. W. Coley, R. Barzilay, MolScribe: Robust Molecular Structure Recognition with Image-to-Graph Generation. *J. Chem. Inf. Model.* 63, 1925–1934 (2023).

25. J. Li, D. Zhang, X. Wang, Z. Hao, J. Lei, Q. Tan, C. Zhou, W. Liu, Y. Yang, X. Xiong, W. Wang, Z. Chen, W. Wang, W. Li, S. Zhang, M. Su, W. Ouyang, Y. Li, D. Zhou, ChemVLM: Exploring the Power of Multimodal Large Language Models in Chemistry Area. *arXiv arXiv:2408.07246 [Preprint]* (2024). <https://doi.org/10.48550/arXiv.2408.07246>.

26. Z. Zhao, B. Chen, J. Li, L. Chen, L. Wen, P. Wang, Z. Zhu, D. Zhang, Z. Wan, Y. Li, Z. Dai, X. Chen, K. Yu, ChemDFM-X: Towards Large Multimodal Model for Chemistry. *Sci. China Inf. Sci* 67, 220109 (2024).

27. D. M. Wilary, J. M. Cole, ReactionDataExtractor: A Tool for Automated Extraction of Information from Chemical Reaction Schemes. *J. Chem. Inf. Model.* 61, 4962–4974 (2021).

28. D. M. Wilary, J. M. Cole, ReactionDataExtractor 2.0: A Deep Learning Approach for Data Extraction from Chemical Reaction Schemes. *J. Chem. Inf. Model.* 63, 6053–6067 (2023).

29. Y. Qian, J. Guo, Z. Tu, C. W. Coley, R. Barzilay, RxnScribe: A Sequence Generation Model for Reaction Diagram Parsing. *J. Chem. Inf. Model.* 63, 4030–4041 (2023).

30. S. R. Vangala, S. R. Krishnan, N. Bung, D. Nandagopal, G. Ramasamy, S. Kumar, S. Sankaran, R. Srinivasan, A. Roy, Suitability of large language models for extraction of high-quality chemical reaction dataset from patent literature. *Journal of Cheminformatics* 16, 131 (2024).

31. J. Dagdelen, A. Dunn, S. Lee, N. Walker, A. S. Rosen, G. Ceder, K. A. Persson, A. Jain, Structured information extraction from scientific text with large language models. *Nat Commun* 15, 1418 (2024).

32. V. Fan, Y. Qian, A. Wang, A. Wang, C. W. Coley, R. Barzilay, OpenChemIE: An Information Extraction Toolkit for Chemistry Literature. *J. Chem. Inf. Model* 64, 5521–5534 (2024).

33. J.-B. Alayrac, J. Donahue, P. Luc, A. Miech, I. Barr, Y. Hasson, K. Lenc, A. Mensch, K. Millican, M. Reynolds, others, Flamingo: a visual language model for few-shot learning. *Advances in neural information processing systems* 35, 23716–23736 (2022).

34. Y. Shen, K. Song, X. Tan, D. Li, W. Lu, Y. Zhuang, Hugginggpt: Solving ai tasks with chatgpt and its friends in hugging face. *Advances in Neural Information Processing Systems* 36 (2024).
35. Z. Yang, L. Li, J. Wang, K. Lin, E. Azarnasab, F. Ahmed, Z. Liu, C. Liu, M. Zeng, L. Wang, Mm-react: Prompting chatgpt for multimodal reasoning and action. *arXiv preprint arXiv:2303.11381* (2023).
36. C. Wu, S. Yin, W. Qi, X. Wang, Z. Tang, N. Duan, Visual chatgpt: Talking, drawing and editing with visual foundation models. *arXiv preprint arXiv:2303.04671* (2023).
37. Z. Liu, Y. He, W. Wang, W. Wang, Y. Wang, S. Chen, Q. Zhang, Y. Yang, Q. Li, J. Yu, others, Internchat: Solving vision-centric tasks by interacting with chatbots beyond language. *arXiv preprint arXiv:2305.05662* (2023).
38. W. Wang, Z. Chen, X. Chen, J. Wu, X. Zhu, G. Zeng, P. Luo, T. Lu, J. Zhou, Y. Qiao, others, Visionllm: Large language model is also an open-ended decoder for vision-centric tasks. *Advances in Neural Information Processing Systems* 36 (2024).
39. K. Chen, Z. Zhang, W. Zeng, R. Zhang, F. Zhu, R. Zhao, Shikra: Unleashing Multimodal LLM's Referential Dialogue Magic. *arXiv preprint arXiv:2306.15195* (2023).
40. S. Zhang, P. Sun, S. Chen, M. Xiao, W. Shao, W. Zhang, Y. Liu, K. Chen, P. Luo, GPT4RoI: Instruction Tuning Large Language Model on Region-of-Interest (2024).
41. Z. Peng, W. Wang, L. Dong, Y. Hao, S. Huang, S. Ma, F. Wei, Kosmos-2: Grounding multimodal large language models to the world. *arXiv preprint arXiv:2306.14824* (2023).
42. A. Yang, B. Yang, B. Zhang, B. Hui, B. Zheng, B. Yu, C. Li, D. Liu, F. Huang, H. Wei, others, Qwen2. 5 technical report. *arXiv preprint arXiv:2412.15115* (2024).
43. J. Achiam, S. Adler, S. Agarwal, L. Ahmad, I. Akkaya, F. L. Aleman, D. Almeida, J. Altenschmidt, S. Altman, S. Anadkat, others, Gpt-4 technical report. *arXiv preprint arXiv:2303.08774* (2023).
44. A. Hurst, A. Lerer, A. P. Goucher, A. Perelman, A. Ramesh, A. Clark, A. Ostrow, A. Welihinda, A. Hayes, A. Radford, others, Gpt-4o system card. *arXiv preprint arXiv:2410.21276* (2024).
45. S. X. Leong, S. Pablo-García, B. Wong, A. Aspuru-Guzik, MERMAid: Universal multimodal mining of chemical reactions from PDFs using vision-language models. *ChemRxiv [Preprint]* (2025). <https://doi.org/10.26434/chemrxiv-2025-8z6h2>.
46. S. X. Leong, S. Pablo-García, Z. Zhang, A. Aspuru-Guzik, Automated electrosynthesis reaction mining with multimodal large language models (MLLMs). *Chemical Science* 15, 17881–17891 (2024).

47. W. Zhang, C. Cui, Y. Zhao, R. Hu, Y. Liu, Y. Zhou, B. An, AgentOrchestra: A Hierarchical Multi-Agent Framework for General-Purpose Task Solving. arXiv arXiv:2506.12508 [Preprint] (2025). <https://doi.org/10.48550/arXiv.2506.12508>.
48. Y. Zhang, R. Sun, Y. Chen, T. Pfister, R. Zhang, S. O. Arik, “Chain of Agents: Large Language Models Collaborating on Long-Context Tasks” (2024); <https://openreview.net/forum?id=LuCLf4BJsr>.
49. M. Ghavamzadeh, S. Mahadevan, R. Makar, Hierarchical Multi-Agent Reinforcement Learning.
50. Federated Control with Hierarchical Multi-Agent Deep Reinforcement Learning - ADS. <https://ui.adsabs.harvard.edu/abs/2017arXiv171208266K/abstract>.
51. Z. Hou, J. Tang, Y. Wang, HALO: Hierarchical Autonomous Logic-Oriented Orchestration for Multi-Agent LLM Systems. arXiv arXiv:2505.13516 [Preprint] (2025). <https://doi.org/10.48550/arXiv.2505.13516>.
52. D. Gao, Z. Li, X. Pan, W. Kuang, Z. Ma, B. Qian, F. Wei, W. Zhang, Y. Xie, D. Chen, L. Yao, H. Peng, Z. Zhang, L. Zhu, C. Cheng, H. Shi, Y. Li, B. Ding, J. Zhou, AgentScope: A Flexible yet Robust Multi-Agent Platform. arXiv arXiv:2402.14034 [Preprint] (2024). <https://doi.org/10.48550/arXiv.2402.14034>.
53. S. Hong, M. Zhuge, J. Chen, X. Zheng, Y. Cheng, C. Zhang, J. Wang, Z. Wang, S. K. S. Yau, Z. Lin, L. Zhou, C. Ran, L. Xiao, C. Wu, J. Schmidhuber, MetaGPT: Meta Programming for A Multi-Agent Collaborative Framework. arXiv arXiv:2308.00352 [Preprint] (2024). <https://doi.org/10.48550/arXiv.2308.00352>.
54. W. Chen, Y. Su, J. Zuo, C. Yang, C. Yuan, C.-M. Chan, H. Yu, Y. Lu, Y.-H. Hung, C. Qian, Y. Qin, X. Cong, R. Xie, Z. Liu, M. Sun, J. Zhou, AgentVerse: Facilitating Multi-Agent Collaboration and Exploring Emergent Behaviors. arXiv arXiv:2308.10848 [Preprint] (2023). <https://doi.org/10.48550/arXiv.2308.10848>.
55. Q. Wu, G. Bansal, J. Zhang, Y. Wu, B. Li, E. Zhu, L. Jiang, X. Zhang, S. Zhang, J. Liu, A. H. Awadallah, R. W. White, D. Burger, C. Wang, AutoGen: Enabling Next-Gen LLM Applications via Multi-Agent Conversation. arXiv arXiv:2308.08155 [Preprint] (2023). <https://doi.org/10.48550/arXiv.2308.08155>.
56. D. M. Flanigan, F. Romanov-Michailidis, N. A. White, T. Rovis, Organocatalytic Reactions Enabled by N-Heterocyclic Carbenes. Chem. Rev. 115, 9307–9387 (2015).
57. Introduction of InternVL 1.5 Series — InternVL. <https://internvl.readthedocs.io/en/latest/internvl1.5/introduction.html>.
58. Llama 3.2: Revolutionizing edge AI and vision with open, customizable models. <https://ai.meta.com/blog/llama-3-2-connect-2024-vision-edge-mobile-devices/>.
59. Qwen2.5-Max: Exploring the Intelligence of Large-scale MoE Model | Qwen. <https://qwenlm.github.io/blog/qwen2.5-max/>.

60. H. Touvron, L. Martin, K. Stone, P. Albert, A. Almahairi, Y. Babaei, N. Bashlykov, S. Batra, P. Bhargava, S. Bhosale, D. Bikel, L. Blecher, C. C. Ferrer, M. Chen, G. Cucurull, D. Esiobu, J. Fernandes, J. Fu, W. Fu, B. Fuller, C. Gao, V. Goswami, N. Goyal, A. Hartshorn, S. Hosseini, R. Hou, H. Inan, M. Kardas, V. Kerkez, M. Khabsa, I. Kloumann, A. Korenev, P. S. Koura, M.-A. Lachaux, T. Lavril, J. Lee, D. Liskovich, Y. Lu, Y. Mao, X. Martinet, T. Mihaylov, P. Mishra, I. Molybog, Y. Nie, A. Poulton, J. Reizenstein, R. Rungta, K. Saladi, A. Schelten, R. Silva, E. M. Smith, R. Subramanian, X. E. Tan, B. Tang, R. Taylor, A. Williams, J. X. Kuan, P. Xu, Z. Yan, I. Zarov, Y. Zhang, A. Fan, M. Kambadur, S. Narang, A. Rodriguez, R. Stojnic, S. Edunov, T. Scialom, Llama 2: Open Foundation and Fine-Tuned Chat Models. arXiv arXiv:2307.09288 [Preprint] (2023). <https://doi.org/10.48550/arXiv.2307.09288>.

61. A. C. Marco, A. F. Myers, S. Graham, P. D'Agostino, K. Apple, The USPTO Patent Assignment Dataset: Descriptions and Analysis.

62. M. Krallinger, F. Leitner, O. Rabal, M. Vazquez, J. Oyarzabal, A. Valencia, CHEMDNER: The drugs and chemical names extraction challenge. *Journal of Cheminformatics* 7, S1 (2015).

63. J. Lee, W. Yoon, S. Kim, D. Kim, S. Kim, C. H. So, J. Kang, BioBERT: a pre-trained biomedical language representation model for biomedical text mining. *Bioinformatics* 36, 1234–1240 (2020).

64. T. Wu, P. Zhan, W. Chen, M. Lin, Q. Qiu, Y. Hu, J. Song, X. Lin, ChemBERTa embeddings and ensemble learning for prediction of density and melting point of deep eutectic solvents with hybrid features. *Computers & Chemical Engineering* 196, 109065 (2025).

65. C. W. Coley, L. Rogers, W. H. Green, K. F. Jensen, SCScore: Synthetic Complexity Learned from a Reaction Corpus. *J. Chem. Inf. Model.* 58, 252–261 (2018).

66. M. Zhong, S. Ouyang, M. Jiang, V. Hu, Y. Jiao, X. Wang, J. Han, “ReactIE: Enhancing Chemical Reaction Extraction with Weak Supervision” in Findings of the Association for Computational Linguistics: ACL 2023, A. Rogers, J. Boyd-Graber, N. Okazaki, Eds. (Association for Computational Linguistics, Toronto, Canada, 2023; <https://aclanthology.org/2023.findings-acl.767/>), pp. 12120–12130.

67. H. Kim, J. Lee, S. Ahn, J. R. Lee, A merged molecular representation learning for molecular properties prediction with a web-based service. *Sci Rep* 11, 11028 (2021).

68. Tesseract documentation, Tesseract OCR. <https://tesseract-ocr.github.io/>.

69. T. Chen, S. Saxena, L. Li, D. J. Fleet, G. Hinton, Pix2seq: A language modeling framework for object detection. arXiv preprint arXiv:2109.10852 (2021).

70. Y. Chen, C. T. Leung, Y. Huang, J. Sun, H. Chen, H. Gao, MolNexTR: a generalized deep learning model for molecular image recognition. *Journal of Cheminformatics* 16, 141 (2024).

71. Y. Chen, C. T. Leung, J. Sun, Y. Huang, L. Li, H. Chen, H. Gao, Towards Large-scale Chemical Reaction Image Parsing via a Multimodal Large Language Model. arXiv arXiv:2503.08156 [Preprint] (2025). <https://doi.org/10.48550/arXiv.2503.08156>.
72. G. Chen, S. Dong, Y. Shu, G. Zhang, J. Sesay, B. Karlsson, J. Fu, Y. Shi, “AutoAgents: a framework for automatic agent generation” in Proceedings of the Thirty-Third International Joint Conference on Artificial Intelligence (Jeju, Korea, 2024); <https://doi.org/10.24963/ijcai.2024/3> IJCAI ’24, pp. 22–30.

Data availability

All the experiments carried out in this study are available at <https://github.com/CYF2000127/ChemEAGLE>. The full benchmark dataset, model outputs, and annotation files are provided in <https://huggingface.co/datasets/CYF200127/ChemEAGLE>.

Code availability

An open-source version of the ChemEAGLE system is available at <https://github.com/CYF2000127/ChemEAGLE>. This repository contains the complete source code, model interfaces, agent implementation, and instructions for reproducing all experiments described in this study. The online app for ChemEAGLE is accessible at <https://huggingface.co/spaces/CYF200127/ChemEAGLE>, allowing users to directly test and use the system. Access to the proprietary GPT-4o API can be obtained through Azure OpenAI.

Acknowledgments

We thank the Information Technology Services Center (ITSC) in HKUST for providing the HPC3 and SuperPod Cluster as our computational resources.

Funding

We acknowledge the financial support from the Hong Kong University of Science and Technology (Project No. R9251, Z1269).

Author contributions

Conceptualization: YC, LL, HG; Methodology: YC, HG, CTL; Benchmark construction: BY, YC; Computational experiments and code development: YC, CTL, BY; Visualization: YC, CTL; Project administration: HG; Supervision: HG, HC, JS, YH; Writing – original draft: YC, CTL; Writing – review & editing: YC, CTL, LL, HG.

Competing interests

Authors declare that they have no competing interests.

Supplementary information

Supplementary Notes 1 to 15

Figs. S1 to S9

Tables S1 to S5

References

Supplementary Information for

A Multi-Agent System Enables Versatile Information Extraction from the Chemical Literature

Yufan Chen, Ching Ting Leung, Bowen Yu, Jianwei Sun, Yong Huang,
Linyan Li, Hao Chen, Hanyu Gao

Corresponding author: Hanyu Gao, hanyugao@ust.hk

The Supplementary Information includes:

Supplementary Notes 1 to 15
Figs. S1 to S9
Tables S1 to S5
References

Supplementary Notes

Supplementary Note 1: Details of ChemEAGLE's extraction plan for multimodal reaction graphics with text-based tables

This section details the practical extraction plan of ChemEAGLE when handling multimodal reaction graphics accompanied by text-based tables, as shown in Fig. S2. While the overall agent-based modular framework remains consistent, the workflow adapts to the distinctive requirements of text-based substitution tables.

Upon receiving a reaction image with an associated text-based table, ChemEAGLE's Planner agent, first determines the content type and orchestrates the agent pipeline of the plan. The Reaction template parsing agent extracts the core molecular framework and SMILES representations for all template reactants and products using RxnImgParser and Image2Graph, correcting OCR and R-group placeholders as needed. Next, the Text-based R-group substitution agent plays a central role. It applies the TableParser tool to extract explicit R-group assignments and substituent details from the table, row by row. These extracted R-groups are then used to systematically replace placeholders in the reaction template, reconstructing all possible reactant and product variants. The Graph2SMILES tool is subsequently called to generate canonical SMILES strings for each reconstructed variant, ensuring that the structural diversity specified in the table is fully realized. The Condition interpretation agent then extracts and categorizes experimental details (e.g., reagents, solvents, temperature, yields) using TesseractOCR and RxnConInterpreter, and aligns these conditions to the correct variant based on table entries or footnotes. Meanwhile, the Text extraction agent identifies and extracts supplementary reaction information from any descriptive text or captions present in the image, leveraging OCR and NER tools. This allows for the capture and integration of additional context (such as abbreviations, specific reagents, or experimental remarks) that may not be represented in the table or main diagram. Finally, the Data structure agent integrates all extracted information into a unified JSON record. This record provides a complete, structured representation of every reaction variant defined in the text-based table, ready for downstream database inclusion or automated analysis.

Compared to the extraction plan for structure-based tables, the key difference here is the focus on systematic parsing and row-wise substitution of table-defined R-groups, as well as the alignment of table-driven metadata with molecular representations. By modularizing these steps and leveraging agent collaboration, ChemEAGLE achieves robust, accurate, and scalable extraction from complex multimodal graphics featuring text-based tables.

Supplementary Note 2: Details of ChemEAGLE’s extraction plans for single-modal sub-tasks

This section illustrate how the Planner agent in ChemEAGLE dynamically devises extraction plans for four representative chemical information extraction sub-tasks, according to the input modality and style.

For molecular image recognition, Planner activates only the Molecular recognition agent and Data structure agent. Upon receiving a molecular image, the Molecular recognition agent applies visual detection tools (MolDetector, Image2Graph, Graph2SMILES) to segment, interpret, and convert all molecules within the image into canonical SMILES strings. The Data structure agent then standardizes and outputs the results as a structured molecular list.

In reaction image parsing, the workflow involves the Reaction template parsing agent, Condition interpretation agent, and Data structure agent. The input reaction image is first parsed for template molecules and placeholders; R-group substitutions are resolved if present. Simultaneously, the Condition interpretation agent extracts and classifies all textual condition information (reagents, solvents, temperature, time, yield) from the image. All reaction and condition elements are finally assembled by the Data structure agent into a comprehensive, machine-readable reaction record.

For named entity recognition, ChemEAGLE uses the Text extraction agent and Data structure agent. The Text extraction agent leverages advanced NER tools to identify and classify chemical entities in the input text into specific categories (such as SYSTEMATIC, IDENTIFIERS, FAMILY, etc.), which are then compiled by the Data structure agent for downstream use or analysis.

In text-based reaction extraction, the Planner again deploys the Text extraction agent and Data structure agent. Here, the workflow is focused on parsing scientific paragraphs to extract not only chemical entities but also explicit reaction roles and structures. The Text extraction agent uses specialized extraction tools to identify reactants, products, reagents, and reaction conditions from textual data. These are then standardized and output in a structured format.

Supplementary Note 3: Implementation details of MolDetector

The MolDetector was trained on a dataset of 1800 annotated reaction diagrams, originally collected for our prior work. For detection, annotations include bounding boxes for all molecule entities, while coreference training utilizes additional identifier boxes and explicit coreference annotations. The dataset was split into 1250 images for training, 200 for validation, and 350 for testing.

The architecture for MolDetector is based on a ResNet-50 (1) encoder with a 4-layer Transformer (2) decoder, inspired by the Pix2Seq (3) framework and implemented using HuggingFace's BERT library. Prior to fine-tuning, the model was pretrained for 300 epochs on the MS-COCO dataset to strengthen its general detection capabilities. Fine-tuning was then performed for 200 epochs each on the detection and coreference tasks, using a batch size of 32, a fixed input resolution of 1333×1333 , and a maximum learning rate of 0.0001 with a linear warmup over the first 2% of steps. Model training was conducted using two NVIDIA 4090 GPUs. At inference time, post-processing steps remove duplicate and degenerate bounding boxes to ensure high-quality detections.

Supplementary Note 4: Implementation details of MolNER

The MolNER model is based on a fine-tuned BioBERT-Large architecture (4), selected for its proven effectiveness in biomedical and chemical entity recognition tasks. ChemNER was trained using the CHEMDNER corpus, which contains manually annotated abstracts from high-impact chemistry journals. The annotated entities in the dataset are classified into seven categories: SYSTEMATIC, IDENTIFIERS, FORMULA, TRIVIAL, ABBREVIATION, FAMILY, and MULTIPLE. For our experiments, we followed the official train-test split of the CHEMDNER corpus: 3,500 samples (29,478 mentions) for training and 3,000 samples (25,351 mentions) for testing. The annotated entity spans were converted into IOB2 tagging format after tokenization.

Model training was performed in PyTorch for 50 epochs, using a maximum learning rate of 0.0001 and a batch size of 32. Training was conducted on a Linux server equipped with 48 CPUs, 100GB RAM, and ten NVIDIA 3090 GPUs. The BioBERT-Large model checkpoint was further fine-tuned on the CHEMDNER dataset under these conditions to optimize performance for chemical named entity recognition.

Supplementary Note 5: Implementation details of ChemRxnExtractor

ChemRxnExtractor (5) is a rule- and machine learning-based pipeline designed to extract and structure chemical reactions from text. The system operates in several stages. First, plain text is obtained either directly from digital documents or by applying an OCR engine to scanned literature. Sentences are split into manageable segments using heuristics and chemical-aware sentence splitting routines. Chemical named entities are then identified and normalized using dictionary lookups and regular expressions, supplemented by a fine-tuned BiLSTM-CRF model for named entity recognition (NER), trained on the CHEMDNER and related corpora.

Next, ChemRxnExtractor applies a hybrid sequence labeling and template matching approach to detect reaction mentions. Candidate reaction sentences are further processed to assign roles (reactant, product, reagent, etc.) using a supervised classification model trained on annotated chemical reaction datasets. The system also resolves entity coreferences where possible, linking molecule abbreviations and systematic names to the correct structures in the reaction.

For training, ChemRxnExtractor utilizes a corpus with manually annotated chemical reactions and entity mentions in ~200,000 published articles. The NER and role labeling models are implemented in PyTorch, and are trained using cross-entropy loss with early stopping based on validation set performance. All preprocessing and postprocessing routines are written in Python, and the full system is designed for efficient batch processing of long documents, supporting both PDF and plain text inputs. At inference, ChemRxnExtractor takes as input paragraphs or documents, and outputs structured JSON objects detailing all extracted reactions, with roles, condition mentions, and page/paragraph context.

Supplementary Note 6: Implementation details of Image2Graph

Image2Graph is built upon the MolNexTR architecture (6), which employs a dual-stream encoder-decoder design to robustly convert chemical structure images into molecular graphs. The encoder consists of two parallel streams: a ConvNext-based (7) CNN for capturing local, short-range features, and a multi-scale Vision Transformer (ViT) (8) stream for encoding long-range dependencies across the image. The ConvNext backbone is initialized from ImageNet-pretrained weights, producing hierarchical feature maps at four resolutions (from 1/4 to 1/32 of the input). The ViT stream applies four parallel transformer blocks, each processing different feature scales via patch embedding and transformer encoding layers, then concatenates their outputs for holistic image understanding.

The structure decoder is a six-layer transformer with eight attention heads, a hidden size of 256, and sinusoidal position encoding. It follows a two-stage autoregressive sequence prediction process: first, the model predicts a sequence of atom types and their 2D coordinates; second, it predicts bond types for all possible atom pairs. All tokens are generated conditionally and autoregressively. Atom tokens encode atom type (including element symbol, charge, and hydrogen count) and spatial coordinates. Bond tokens specify bond type ("single", "double", "triple", "aromatic", "solid wedge", "dashed wedge", or "None") for each atom pair. This architecture allows Image2Graph to achieve strong robustness to image style variation, graphical noise, and ambiguous or abbreviated atom labels

For training, the model used a combination of synthetic and real-world data to maximize the model's generalization. The synthetic portion includes 1 million rendered images randomly sampled from the PubChem database, while the real data comprises 680,000 molecular images from the USPTO dataset, normalized to 384×384 pixels. Data augmentation is applied, including random rotations and diverse drawing styles. Training uses the Adam optimizer with a maximum learning rate of 0.0003, a linear warmup for 5% of steps, and a batch size of 256. The model is trained for 40 epochs on a cluster with ten NVIDIA RTX 3090 GPUs. During inference, the model uses beam search to decode atom and bond sequences.

Supplementary Note 7: Implementation details of Graph2SMILES

The core function of Graph2SMILES takes as input the 2D coordinates of atoms, a list of atom symbols (including explicit R-group placeholders and chemical abbreviations), and the adjacency matrix of bond types.

First, Graph2SMILES initializes an editable RDKit molecular graph, sequentially adding atoms and bonds according to the input data. Atom symbols are handled with care: recognized abbreviations and R-group labels are mapped to appropriate SMILES fragments or placeholders, while invalid or unknown atoms are replaced with isotopically labeled wildcard atoms to maintain graph integrity. For each bond, the tool assigns the correct order and type (including single, double, triple, aromatic, wedge, and dash bonds). Stereochemistry is inferred using both the provided coordinates and any wedge/dash information. The tool adds 2D conformers, assigns chiral tags from bond directions, and post-processes the molecule to ensure correct assignment of tetrahedral and E/Z stereochemistry where possible. For molecular graphs containing functional groups as abbreviations or condensed formulas, Graph2SMILES attempts to expand these to explicit substructures, using a predefined mapping or by parsing the formula. If expansion is not possible, the original abbreviation is retained as an alias.

After constructing the full molecular graph, the tool sanitizes and canonicalizes the structure, extracting the main connected component if necessary. Finally, it generates the isomeric SMILES string as the output, reporting the success rate of conversion for all processed molecules. All conversion steps are efficiently parallelized, enabling large-scale and robust translation of diverse chemical images into machine-readable SMILES, including complex cases with R-groups, abbreviations, and stereochemistry.

Supplementary Note 8: Implementation details of SMILESReconstructor.

The core idea of the SMILESReconstructor is to leverage the structural relationship between the product template and its variants: for each product variant, the unique R-group substituents are first identified by substructure matching between the variant and the product template.

The detail workflow begins by parsing the input reaction extraction results and product coreference information. The method first determines the main product molecule and locates all R-group sites within the product template using atom symbol inspection and pattern matching. These R-group positions are mapped via atomic indices and recorded for subsequent operations. For each reactant, the tool similarly locates and maps R-group sites, aligning them with those in the product by atom indices. Reactant molecular graphs are re-aligned as needed to match the product template using atom mapping utilities. Next, the tool iterates over all relevant coreference product SMILES entries, searching for labels that match the primary product variant and extracting any annotation-defined R-group substitutions. For each candidate product variant, substructure matching is performed between the product template and the variant, isolating the specific fragments corresponding to each R-group site. Once the R-group fragments are determined, SMILESReconstructor systematically substitutes these fragments into the appropriate positions in the reactant template, rebuilding the complete reactant variant as a valid SMILES string. This includes robust error handling for cases where annotations are ambiguous, molecule formats are inconsistent, or mappings are incomplete.

Throughout the process, auxiliary functions handle label normalization, atom mapping, and fragment expansion. The method also includes checks for special cases (e.g., one-atom reactants, different R-group label schemes, and ambiguous abbreviations), ensuring reliable performance across a wide range of reaction schematics. The final output of SMILESReconstructor is a set of reconstructed full reactant SMILES for each product variant, together with the mapping context.

Supplementary Note 9: Implementation details of RxnImgParser and RxnConInterpreter. RxnImgParser and RxnConInterpreter are two specialized tools built on top of the RxnIM multimodal large language model (MLLM) framework, and are adapted for detailed reaction image parsing and condition interpretation, respectively. Both tools inherit RxnIM’s encoder-decoder architecture, which integrates visual and language understanding through dedicated modules, and they share a common set of model components and training strategies.

Both tools use a unified encoder-decoder architecture: a ResNet-50 (1) image encoder and a BERT-Base (9) text encoder extract multi-scale visual and textual features, which are fused via cross-attention. A deformable DETR (10) module tokenizes image features, enabling precise localization and segmentation of molecular structures and condition regions. The task decoder is based on Llama-2-7B (11), which has been expanded to recognize special tokens relevant to reaction parsing (such as [Str], [Txt], [Rxn/st], [Cnd/st], [Agt], [Svt], etc.). For RxnImgParser, the output is structured as a set of reaction sequences, each with detailed object categories, coordinates, and roles (reactant, condition, product). RxnConInterpreter focuses on extracting condition text, assigning role labels such as reagent, solvent, temperature, time, and yield to each detected word.

Training of RxnImgParser and RxnConInterpreter is jointly performed in three stages: (1) training the encoder and D-DETR on conventional object detection; (2) joint fine-tuning on synthetic reaction images for component identification and condition extraction; and (3) final fine-tuning of the LLM decoder on real-world images. AdamW optimizer and cosine learning rate schedule are used, and all training is done on 8 NVIDIA H800 GPUs.

Supplementary Note 10: Implementation details of Reaction template parsing agent

The implementation of the Reaction template parsing agent is organized as a sequential multi-tool pipeline, using GPT-4o (12) as the central reasoning MLLM (see **Fig. S4**). Upon receiving an input reaction graphic, the agent uses GPT-4o to guide the RxnImgParser tool, which segments all relevant molecular regions, such as reactants, products, and other chemical components, by assigning bounding boxes based on visual and spatial cues present in the image.

For each detected region, GPT-4o instructs the application of Image2Graph, extracting detailed molecular graph representations. At this stage, any R-group placeholders (such as [Ar2]) present in the molecule are preserved for downstream processing. A critical implementation step involves the accurate handling of R-group annotations and substitutions: GPT-4o parses all annotation text (such as equations like "Ar₂ = 2-ClC₆H₄") using a combination of rule-based string matching and contextual language understanding, establishing explicit mappings between placeholder labels and their corresponding R-group fragments.

GPT-4o then directs the agent to scan the atom sets in each molecular graph and replace any placeholder labels with the correct chemical fragments. This substitution phase is tightly coupled with robust error correction: GPT-4o leverages both contextual visual cues and language-based heuristics to correct for OCR errors, font mismatches, or ambiguous handwriting, significantly increasing resilience to real-world noise. Once all molecular graphs are updated with explicit R-group substitutions, GPT-4o invokes Graph2SMILES to convert the completed graphs into canonical SMILES strings, ensuring that both original structures and substituted R-groups are encoded in a machine-readable format for downstream computational use.

Finally, GPT-4o organizes the extracted information into a standardized JSON record, containing reaction templates, reactant and product SMILES, and relevant annotation metadata. Optionally, the agent can preserve intermediate results such as bounding boxes, graph objects, and preliminary SMILES outputs for debugging or audit. The integration of GPT-4o enables the Reaction Template Parsing Agent to flexibly handle diverse graphical layouts and annotation styles, ensuring both robustness and accuracy in reaction extraction from complex chemical graphics.

Supplementary Note 11: Implementation details of Molecular recognition agent

The Molecular recognition agent is implemented as a modular pipeline that leverages GPT-4o as its core reasoning engine, as illustrated in **Fig. S5**. At each step, GPT-4o not only guides the invocation of the extraction tools but also interprets intermediate results and coordinates subsequent actions based on the contextual information present in the image.

The workflow begins with the MolDetector tool, which is orchestrated by GPT-4o to scan the input image and localize all molecular structures. GPT-4o parses the output to ensure that even in complex layouts with overlapping or densely packed molecules, every candidate molecular region is identified.

For each detected region, GPT-4o directs the use of Image2Graph to convert the visual structure into a detailed chemical graph. If a molecule already includes explicit textual coreferences (such as “3a,” “product,” or “B17”), GPT-4o recognizes and extracts these coreferences directly without further inference, ensuring that native annotations from the graphic are retained and assigned to the correct molecule in the output. Next, GPT-4o systematically examines the image for R-group formulas, equations, or special annotations, such as “Ar2 = 2-ClC6H4.” If placeholders (like [Ar2]) are present in the atom set, GPT-4o coordinates the substitution of these placeholders with the correct explicit fragments. In this step, GPT-4o also applies its vision-language reasoning to resolve OCR or font recognition errors using context from the image, ensuring accurate chemical identity and structure.

After all substitutions and corrections, GPT-4o calls Graph2SMILES to convert the updated molecular graphs into standardized SMILES strings. This is followed by the agent labeling each molecule’s type (reactant, product, template, condition, etc.), making the output ready for downstream processing or integration into full reaction records. Throughout this process, GPT-4o’s multimodal reasoning capabilities allow the agent to adaptively handle diverse annotation styles, graphical conventions, and edge cases in real chemical literature. By explicitly retaining native molecular labels when present, and using advanced language-vision inference for annotation and correction, the Molecular Recognition Agent achieves both robustness and fidelity in extracting molecular information from complex chemical graphics.

Supplementary Note 12: Implementation details of Structure-based R-group substitution agent

The implementation of the Structure-based R-group substitution agent centers around leveraging both the output of the reaction template parsing agent and the molecular recognition agent to achieve robust, automated reconstruction of all reaction variants present in complex reaction graphics, as illustrated in **Fig. S6**. Upon receiving as input the parsed reaction template (containing the general scaffold with R-group placeholders) and the set of extracted product variant structures (provided as SMILES), the agent performs systematic substructure matching using the SMILESReconstructor tool and GPT-4o-based agent reasoning.

In practice, for each product variant, the agent identifies the core scaffold shared with the reaction template and isolates the unique R-group fragments present in the product structure but absent in the template. This step is critical for precisely mapping variant-specific modifications, such as different substituents or functional groups, back to their correct positions in the reactant scaffold. The agent then substitutes these R-group SMILES fragments into the appropriate sites of the reactant template, thus reconstructing the corresponding full reactant SMILES for each reaction variant. Another key technical advantage of this implementation is its flexibility in handling complex or partially labeled graphics. Even when explicit molecular coreferences are absent or R-group sites are only indirectly indicated, the agent utilizes chemical graph analysis and MLLM-based reasoning to accurately pair variants with templates. Furthermore, the GPT-4o-based workflow ensures that the entire process from substructure identification to SMILES reconstruction is performed in a context-aware and error-tolerant manner, reducing the risk of mismatches or missed variants.

The final output is a comprehensive list of full reaction SMILES for each variant, paired with their respective reaction conditions and metadata, ready for downstream extraction or analysis. By systematically automating this traditionally labor-intensive process, the Structure-based R-group substitution agent enables ChemEAGLE to achieve both high accuracy and scalability in multimodal chemical data extraction.

Supplementary Note 13: Implementation details of Text-based R-group substitution agent

The Text-based R-group substitution agent is engineered to efficiently process reaction images that are paired with text-based tables detailing R-group substitutions, as illustrated in **Fig. S7**. Its workflow begins by gathering the intermediate outputs generated by the Reaction template parsing agent and the Molecular recognition agent. Specifically, the agent first applies the TableParser tool, under the orchestration of the GPT-4o-powered agent, which systematically extracts R-group substitution information from the table. This extraction step identifies the correspondence between R-group labels (such as R1, R2, etc.) and their specific substituent values for each variant, row by row.

Once the mapping of R-groups is established, the agent programmatically traverses the molecular graphs of both reactants and products (produced in earlier steps), replacing any placeholder atoms (e.g., "[R1]", "[R2]") with the actual substituent groups specified in the table. This row-wise substitution ensures that every molecular structure accurately reflects the intended chemical variant for each entry in the table, regardless of how many positions are substituted simultaneously. After the substitution, the agent calls the Graph2SMILES tool for each updated molecular graph, converting them into canonical SMILES strings. The agent then assembles the complete set of reaction SMILES for all variants, mapping each entry back to its associated row in the table and preserving all extracted metadata (such as yields, times, or special notes).

A notable implementation detail is the agent's ability to handle complicated tables, including those with missing data, alternative conditions, or multi-level R-group sets, by leveraging both explicit table structure and contextual cues extracted via GPT-4o. This allows the agent to robustly process a broad range of real-world chemical tables found in published reaction graphics, making ChemEAGLE's approach broadly applicable to diverse extraction scenarios.

The final output is a standardized JSON object containing all variant-specific reaction SMILES, ready for integration with downstream analyses or databases. Intermediate substitution mappings and any detected table inconsistencies can be optionally logged for quality control or error correction.

Supplementary Note 14: Implementation details of Condition interpretation agent

The Condition interpretation agent in ChemEAGLE is designed to systematically extract, interpret, and structure reaction condition information from chemical images that present text-based experimental details, as shown in **Fig. S8**. The implementation begins with the application of the TesseractOCR tool, under the control of the GPT-4o-powered agent, to extract all visible text regions within the reaction graphic. This OCR step recovers raw condition annotations such as reagent amounts, solvent names, temperature, yield ranges, and any additional experimental notes or qualifiers.

Following text extraction, the agent invokes the RxnConInterpreter tool to semantically parse and classify each piece of extracted text into a structured set of roles. These include explicit categories such as "reagent", "solvent", "temperature", "yield", "time", and "add_info". The role assignment relies on a combination of keyword pattern matching and context-aware heuristics, leveraging GPT-4o's reasoning to resolve ambiguous or partially recognized phrases. When possible, chemical structures detected in the image (e.g., specific molecules linked to reagents or conditions) are also mapped to SMILES strings or explicit labels, ensuring chemical identity is preserved.

A crucial implementation feature is the alignment of extracted condition roles with specific reactions or molecular variants present in the graphic. The agent matches each condition annotation to its corresponding reaction entry, often using spatial proximity, reference labels, or row/column logic inferred from the layout of the image and tables. This ensures that conditions such as yields or specific reagents are correctly attributed to the proper reaction variant when multiple reactions or conditions are shown in the graphics.

The resulting output is a structured, hierarchical condition list in JSON format, mapping all detected and interpreted reaction conditions to their respective reactions and chemical entities. Intermediate results, such as OCR confidence scores or unresolved annotations, may also be logged for error analysis or further manual review. This stepwise and modular approach allows ChemEAGLE to handle a broad spectrum of reaction graphics, ranging from simple, single-reaction schemes to densely annotated multi-row scope tables, delivering comprehensive and accurate extraction of experimental context for downstream data use.

Supplementary Note 15: Implementation details of Text extraction agent

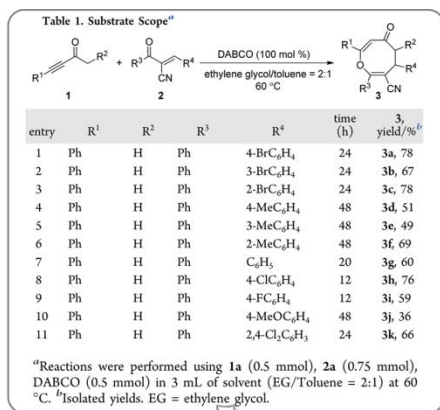
The Text extraction agent in ChemEAGLE is engineered to robustly extract and structure chemical reaction information from the textual content associated with reaction images, as illustrated in **Fig. S9**. Upon receiving a chemical graphic, the agent first employs TesseractOCR under GPT-4o orchestration to digitize all text segments within the image, recovering textual reaction descriptions, experimental footnotes, and relevant figure captions. If the input is already provided in text form, this step is skipped.

Once the text is extracted, the agent sequentially invokes two specialized natural language processing tools: MolNER and ChemRxnExtractor. MolNER performs chemical named entity recognition (NER), tagging chemical names, abbreviations, and systematic identifiers within the recovered text and assigning them to appropriate classes such as SYSTEMATIC, IDENTIFIERS, or ABBREVIATION. This high-fidelity recognition step is essential for downstream linking and accurate mapping of textual entities to chemical structures. The ChemRxnExtractor tool is then called to parse the entity-tagged text, extracting structured reaction components including reactants, products, reagents, and associated conditions. This tool leverages deep learning-based extraction models to map the semantic roles of each chemical mention and to construct a structured reaction record.

A key implementation step involves multimodal alignment: the agent checks if chemical entities or abbreviations mentioned in the text correspond to graphical elements, such as molecule structures or R-group fragments, previously extracted from images or tables. If a chemical (e.g., "B27") is referenced in both text and graphics, the agent ensures their information is cross-linked. This may include merging SMILES structures, identifiers, and condition roles into the unified text extraction output.

The final output is a harmonized JSON object that encapsulates all recognized chemical entities, reactions, and their roles, along with their cross-modal relationships. The process is modular and transparent, allowing intermediate outputs such as raw OCR text, NER labels, and extracted reaction roles to be reviewed or audited as needed. This layered and agent-driven workflow enables ChemEAGLE to support highly reliable, multi-source extraction, which is critical for building structured chemical knowledge bases from unstructured literature.

Supplementary Figures



^aReactions were performed using **1a** (0.5 mmol), **2a** (0.75 mmol), DABCO (0.5 mmol) in 3 mL of solvent (EG/Toluene = 2:1) at 60 °C. ^bIsolated yields. EG = ethylene glycol.

Plan

Extraction Plan for *Multimodal Reaction Graphics* with Text-based Table



Actions



Reaction template parsing agent

Fig. S1. Extraction plan of ChemEAGLE's multi-agent system for multimodal reaction graphics with text-based tables. Unlike the structure-based table scenario, no explicit product variant structures need to be detected here. ChemEAGLE's planner therefore skips the Molecular recognition agent and invokes the Text-based R-group substitution agent (rather than the Structure-based R-group substitution agent) to graft the detailed R-group definitions directly into the reaction template.

Full Reaction List

```

{"reactions": [
  {"reaction_id": "0_1", # Reaction Template
    "reactants": [{"smiles": "C(=O)(C=C[R1])[R2]", "label": "1"}, {"smiles": "C(C#N)=C[R3])[R4]", "label": "2"}], "conditions": [{"role": "reagent", "text": "DABCO (100 mol%)"}, {"role": "solvent", "text": "ethylene glycol/toluene"}, {"role": "temperature", "text": "60 °C"}], "products": [{"smiles": "C1(C(=O)[R1])C([R3])(CN)C(=O)[R4]C=C1", "label": "3"}]}, {"reaction_id": "1_1", # Detailed Reaction
    "reactants": [{"smiles": "c1ccccc1C(=O)C=CH", "label": "1a"}, {"smiles": "c1ccc(Br)cc1C(C#N)=c1ccccc1", "label": "2a"}], "conditions": [{"role": "reagent", "text": "DABCO (100 mol%)"}, {"role": "solvent", "text": "ethylene glycol/toluene"}, {"role": "temperature", "text": "60 °C"}, {"role": "yield", "text": "78%"}, {"role": "time", "text": "24h"}], "products": [{"smiles": "c1ccccc1C1(c1ccccc1CN)C(C(=O)c1ccc(Br)cc1)=C1O", "label": "3a"}]}, #More reactions ],
  "text_extraction": ["Reaction were performed using 1a (0.5 mmol)[reactant][IDENTIFIERS], 2a (0.75 mmol)[reactant][IDENTIFIERS], DABCO[reagent][ABBREVIATION]. \n"]
]

```

```

1  {"reactions": [
2    {"reaction_id": "0_1", "reactants": [{"smiles": "[Ar]C([R])=O", "label": "1"}, {"smiles": "Cc1ccc(S(=O)(=O)N2O2c2cccc2Cl)cc1", "label": "2"}], "conditions": [{"role": "reagent", "text": "10 mol% B17 or B27", "smiles": "C(=C=C1=C1C[N+]=2CN3[C@H](C(C1=CC(=CC=C1)(C5=CC=CC=C5)O[Si](C)(C)C(C)(C)CCC3=N2.F[B-](F)(F)F", "label": "B17"}], "products": [{"smiles": "[Cs+].[Cs-].[O-]C(=O)[O-]"}], {"role": "solvent", "text": "PhMe", "smiles": "Cc1cccc1"}, {"role": "temperature", "text": "rt"}, {"role": "yield", "text": "88 - 78%"}], "products": [{"smiles": "[Ar]C1([R])O[C@H](c2cccc2Cl)N(S(=O)(=O)c2ccc(C)cc2)C1=O", "label": "3"}]}, {"reaction_id": "1_1", "reactants": [{"smiles": "CCC(=O)c1cccc1", "label": "1a"}, {"smiles": "Cc1ccc(S(=O)(=O)N2O2c2cccc2Cl)cc1", "label": "2a"}], "conditions": [{"role": "reagent", "text": "10 mol% B17 or B27", "smiles": "C(=C=C1=C1C[N+]=2CN3[C@H](C(C4=CC=CC=C4)(C5=CC=CC=C5)O[Si](C)(C)C(C)(C)CCC3=N2.F[B-](F)(F)F", "label": "B27"}], "products": [{"smiles": "[Cs+].[Cs-].[O-]C(=O)[O-]"}], {"role": "solvent", "text": "PhMe", "smiles": "Cc1cccc1"}, {"role": "temperature", "text": "rt"}, {"role": "yield", "text": "78%"}], "products": [{"smiles": "[Ar]C1([R])O[C@H](c2cccc2Cl)N(S(=O)(=O)c2ccc(C)cc2)C1=O", "label": "3"}]}, {"reaction_id": "2_1", "reactants": [{"smiles": "CCC(=O)c1cccc1", "label": "1b"}, {"smiles": "Cc1ccc(S(=O)(=O)N2O2c2cccc2Cl)cc1", "label": "2b"}], "conditions": [{"role": "reagent", "text": "10 mol% B17 or B27", "smiles": "C(=C=C1=C1C[N+]=2CN3[C@H](C(C4=CC=CC=C4)(C5=CC=CC=C5)O[Si](C)(C)C(C)(C)CCC3=N2.F[B-](F)(F)F", "label": "B17"}], "products": [{"smiles": "[Cs+].[Cs-].[O-]C(=O)[O-]"}], {"role": "solvent", "text": "PhMe", "smiles": "Cc1cccc1"}, {"role": "temperature", "text": "rt"}, {"role": "yield", "text": "71%"}], "products": [{"smiles": "[CC@C](1c2cccc2Cl)O[C@H](c2cccc2Cl)N(S(=O)(=O)c2ccc(C)cc2)C1=O", "label": "3a"}], {"additional_info": [{"text": "14:1 dr, 91% ee"}]}, {"reaction_id": "3_1", "reactants": [{"smiles": "CCC(=O)c1cccc1", "label": "1b"}, {"smiles": "Cc1ccc(S(=O)(=O)N2O2c2cccc2Cl)cc1", "label": "2b"}], "conditions": [{"role": "reagent", "text": "10 mol% B17 or B27", "smiles": "C(=C=C1=C1C[N+]=2CN3[C@H](C(C4=CC=CC=C4)(C5=CC=CC=C5)O[Si](C)(C)C(C)(C)CCC3=N2.F[B-](F)(F)F", "label": "B17"}], "products": [{"smiles": "[Cs+].[Cs-].[O-]C(=O)[O-]"}], {"role": "solvent", "text": "PhMe", "smiles": "Cc1cccc1"}, {"role": "temperature", "text": "rt"}, {"role": "yield", "text": "60%"}], "products": [{"smiles": "[CC@C](1c2cccc2Cl)O[C@H](c2cccc2Cl)N(S(=O)(=O)c2ccc(C)cc2)C1=O", "label": "3b"}], {"additional_info": [{"text": "14:1 dr, 92% ee"}]}, {"reaction_id": "4_1", "reactants": [{"smiles": "CCCC(=O)c1ccc(Br)cc1", "label": "1d"}, {"smiles": "Cc1ccc(S(=O)(=O)N2O2c2cccc2Cl)cc1", "label": "2d"}], "conditions": [{"role": "reagent", "text": "10 mol% B17 or B27", "smiles": "C(=C=C1=C1C[N+]=2CN3[C@H](C(C4=CC=CC=C4)(C5=CC=CC=C5)O[Si](C)(C)C(C)(C)CCC3=N2.F[B-](F)(F)F", "label": "B17"}], "products": [{"smiles": "[Cs+].[Cs-].[O-]C(=O)[O-]"}], {"role": "solvent", "text": "PhMe", "smiles": "Cc1cccc1"}, {"role": "temperature", "text": "rt"}, {"role": "yield", "text": "78%"}], "products": [{"smiles": "[CC@C](1c2ccc(Br)cc2)O[C@H](c2cccc2Cl)N(S(=O)(=O)c2ccc(C)cc2)C1=O", "label": "3c"}], {"additional_info": [{"text": "14:1 dr, 91% ee"}]}, {"reaction_id": "5_1", "reactants": [{"smiles": "CC(=O)c1cccc1", "label": "1e"}, {"smiles": "Cc1ccc(S(=O)(=O)N2O2c2cccc2Cl)cc1", "label": "2e"}], "conditions": [{"role": "reagent", "text": "10 mol% B17 or B27", "smiles": "C(=C=C1=C1C[N+]=2CN3[C@H](C(C4=CC=CC=C4)(C5=CC=CC=C5)O[Si](C)(C)C(C)(C)CCC3=N2.F[B-](F)(F)F", "label": "B17"}], "products": [{"smiles": "[Cs+].[Cs-].[O-]C(=O)[O-]"}], {"role": "solvent", "text": "PhMe", "smiles": "Cc1cccc1"}, {"role": "temperature", "text": "rt"}, {"role": "yield", "text": "61%"}], "products": [{"smiles": "Cc1ccc(S(=O)(=O)N2O2c2cccc2Cl)cc1", "label": "3e"}], {"additional_info": [{"text": "15:1 dr, 85% ee"}]}, {"reaction_id": "6_1", "reactants": [{"smiles": "CCC(=O)c1cccc1", "label": "1f"}, {"smiles": "Cc1ccc(S(=O)(=O)N2O2c2cccc2Cl)cc1", "label": "2f"}], "conditions": [{"role": "reagent", "text": "10 mol% B17 or B27", "smiles": "C(=C=C1=C1C[N+]=2CN3[C@H](C(C4=CC=CC=C4)(C5=CC=CC=C5)O[Si](C)(C)C(C)(C)CCC3=N2.F[B-](F)(F)F", "label": "B17"}], "products": [{"smiles": "[Cs+].[Cs-].[O-]C(=O)[O-]"}], {"role": "solvent", "text": "PhMe", "smiles": "Cc1cccc1"}, {"role": "temperature", "text": "rt"}, {"role": "yield", "text": "52%"}], "products": [{"smiles": "Cc1ccc(S(=O)(=O)N2O2c2cccc2Cl)cc1", "label": "3f"}], {"additional_info": [{"text": "10.1 dr, 94% ee"}]}], "Text description": ["In 2010, an enantioselective formal [3+2] cycloaddition of NHC-bound azolium enolates [reactant][MULTIPLE] and oxaziridines [reactant][SYSTEMATIC] was described by Ye and co-workers. Aryl(alkyl)-disubstituted ketenes were used as precursors of azolium enolates [reactant]. A bifunctional NHC [ABBREVIATION] catalyst B27 [reactant] [IDENTIFIERS] [SMILES:CCCC(=C=C1)(C1[N+]=2CN3[C@H](C(C1=CC(=CC=C1)(C5=CC=CC=C5)O[Si](C)(C)C(C)(C)CCC3=N2.F[B-](F)(F)F bearing a free hydroxyl group was employed."}]}

```

Fig. S2. Complete JSON output of ChemEAGLE on Fig. 3A. ChemEAGLE outputs a complete JSON entry in which every variant reaction (7/7) is present, and each reactant, product, R-group substitution and condition is correct.

```

1  {"reaction_template":
2  {"smiles":"[Ar1]C(=O)[R1].[Ar2]N1C(C=O)N1S(=O)(=O)[R2]>[C@H]([R1])C(=O)N3CC(C=O))[N]S(=O)(=O)[R2]C3[Ar2]", "smarts":"[Ar1:1]C(=O)[C:2].[Ar2:3]N1CC
(=O)N1S(=O)(=O)[R2:4]>>[C@H:2](C(=O)N3CC(C=O)N3S(=O)(=O)[R2:4])[Ar2:3]"}, 
3  "reactions": [{"reaction_id": "1_1", "reactants": [{"smiles": "Clc3cccc3", "label": "1"}, {"smiles": "CC(C(=O)c1cccc1)C(=O)N1CCN(S(=O)(=O)c2ccc(C)cc2)C1", "label": "2"}], "products": [{"smiles": "CC(C(=O)c1cccc1)C(=O)N1CCN(S(=O)(=O)c2ccc(C)cc2)C1", "label": "3a"}, {"smiles": "OC[C@H]1CN(Nic2cc(C(F)(F)F)cc(C(F)(F)F)c2)", "label": "B27"}, {"text": "10 mol% Cs2CO3", "role": "base"}, {"text": "10 mol% Cs2CO3", "role": "yield"}, {"text": "78%", "role": "dr"}, {"text": "14:1", "role": "ee"}, {"text": "91%"}], "condition": [{"role": "reagent", "text": "10 mol% B27"}, {"text": "10 mol% Cs2CO3", "role": "base"}, {"text": "10 mol% Cs2CO3", "role": "yield"}, {"text": "52%", "role": "dr"}, {"text": "15:1", "role": "ee"}, {"text": "85%"}]}, {"reaction_id": "1_2", "reactants": [{"smiles": "Clc3cccc3", "label": "1"}, {"smiles": "CC(C(=O)c1ccc(Br)cc1)C(=O)N1CCN(S(=O)(=O)c2ccc(C)cc2)C1", "label": "2"}], "products": [{"smiles": "CC(C(=O)c1ccc(Br)cc1)C(=O)N1CCN(S(=O)(=O)c2ccc(C)cc2)C1", "label": "3b"}, {"smiles": "OC[C@H]1CN(Nic2cc(C(F)(F)F)cc(C(F)(F)F)c2)", "label": "B27"}, {"text": "10 mol% Cs2CO3", "role": "base"}, {"text": "10 mol% Cs2CO3", "role": "yield"}, {"text": "78%", "role": "dr"}, {"text": "14:1", "role": "ee"}, {"text": "91%"}], "condition": [{"role": "reagent", "text": "10 mol% B27"}, {"text": "10 mol% Cs2CO3", "role": "base"}, {"text": "10 mol% Cs2CO3", "role": "yield"}, {"text": "52%", "role": "dr"}, {"text": "15:1", "role": "ee"}, {"text": "91%"}]}, {"reaction_id": "1_3", "reactants": [{"smiles": "Clc3cccc3", "label": "1"}, {"smiles": "C(C(=O)c1ccc(Cl)cc1)(C)C(=O)N1CCN(S(=O)(=O)c2ccc(C)cc2)C1", "label": "2"}], "products": [{"smiles": "C(C(=O)c1ccc(Cl)cc1)(C)C(=O)N1CCN(S(=O)(=O)c2ccc(C)cc2)C1", "label": "3c"}, {"smiles": "OC[C@H]1CN(Nic2cc(C(F)(F)F)cc(C(F)(F)F)c2)", "label": "B27"}, {"text": "10 mol% Cs2CO3", "role": "base"}, {"text": "10 mol% Cs2CO3", "role": "yield"}, {"text": "60%", "role": "dr"}, {"text": "14:1", "role": "ee"}, {"text": "92%"}], "condition": [{"role": "reagent", "text": "10 mol% B27"}, {"text": "10 mol% Cs2CO3", "role": "base"}, {"text": "10 mol% Cs2CO3", "role": "yield"}, {"text": "60%", "role": "dr"}, {"text": "14:1", "role": "ee"}, {"text": "92%"}]}, {"reaction_id": "1_4", "reactants": [{"smiles": "Clc3cccc3", "label": "1"}, {"smiles": "nPr(C(=O)c1ccc(Cl)cc1)C(=O)N1CCN(S(=O)(=O)c2ccc(C)cc2)C1", "label": "2"}], "products": [{"smiles": "nPr(C(=O)N1CCN(S(=O)(=O)c2ccc(C)cc2)C1)c3ccc(Cl)cc3", "label": "3d"}, {"smiles": "OC[C@H]1CN(Nic2cc(C(F)(F)F)cc(C(F)(F)F)c2)", "label": "B27"}, {"text": "10 mol% Cs2CO3", "role": "base"}, {"text": "10 mol% Cs2CO3", "role": "yield"}, {"text": "60%", "role": "dr"}, {"text": "14:1", "role": "ee"}, {"text": "92%"}], "condition": [{"role": "reagent", "text": "10 mol% B27"}, {"text": "10 mol% Cs2CO3", "role": "base"}, {"text": "10 mol% Cs2CO3", "role": "yield"}, {"text": "60%", "role": "dr"}, {"text": "14:1", "role": "ee"}, {"text": "92%"}]}, {"reaction_id": "1_5", "reactants": [{"smiles": "Clc3cccc3", "label": "1"}, {"smiles": "N1CCN(C(Cl)=O)S(=O)(=O)c2ccc(C)cc2.Clc3cccc3", "label": "2"}], "products": [{"smiles": "CC(C(=O)N1CCN(C(Cl)=O)S(=O)(=O)c2ccc(C)cc2)C(=O)c4cccc5cccc45", "label": "3f"}, {"smiles": "OC[C@H]1CN(Nic2cc(C(F)(F)F)cc(C(F)(F)F)c2)", "label": "B27"}, {"text": "10 mol% B27", "role": "base"}, {"text": "10 mol% Cs2CO3", "role": "base"}, {"text": "10 mol% Cs2CO3", "role": "yield"}, {"text": "61%", "role": "dr"}, {"text": "10:1", "role": "ee"}, {"text": "94%"}], "condition": [{"role": "reagent", "text": "10 mol% B27"}, {"text": "10 mol% Cs2CO3", "role": "base"}, {"text": "10 mol% Cs2CO3", "role": "yield"}, {"text": "61%", "role": "dr"}, {"text": "10:1", "role": "ee"}, {"text": "94%"}]}]

```

Fig. S3. Complete JSON output of GPT-4o on Fig. 3A. GPT-4o outputs a complete JSON entry in which 6 out of 7 variant reactions is present, but all reactants, products, R-group substitutions are wrong, the condition text interpretations are sometimes correct.

Prompt: You are the reaction template parsing agent, your task is to parse the reaction template in this reaction ...

Thought: I will check this reaction and call tools to parse the reaction template.
Actions: Check the reaction, first call RxnImgParser.

(,,, Run RxnImgParser tool)

Observation: The reactant and product molecules have been extracted.

Thought: I need to run the Image2Graph tool to process each molecule.
Actions: Call Image2Graph.

(,,, Run Image2Graph tool)

Observation: There is still a R-group formula "Ar2 = 2-C1C6H4" in the template.

Thought: I need to replace the R-group placeholder with the R-group formula in the graph atom set, then run the Graph2SMILES tool to get the final SMILES.

Actions: Replace the R-group placeholder with the R-group formula:

$$["C", "[Ar2]", "O", "N", "[Ts]] \longrightarrow ["C", "[2-C1C6H4]", "O", "N", "[Ts]]$$

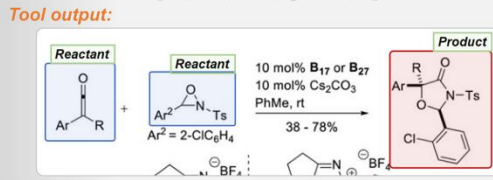
Then Call Graph2SMILES.

(,,, Run Graph2SMILES tool)

Observation: The reaction template SMILES are complete and correct.

Actions: Output the final reaction template SMILES output.

[Tool: RxnImgParser]



[Tool: Image2Graph]

Tool output:

```
{"reactants": [{"Atoms": ["C", "[Ar]", "[R]", "O"], "Bonds": "...", "Coordinates": "..."}, {"Atoms": ["C", "[Ar2]", "O", "N", "[Ts]"], "Bonds": "...", "Coordinates": "..."}], "products": [{"Atoms": ["N", "[Ts]", "C", "O", "[C@H]", "[R]", "[Ar]", "O", "[C@@H]", "C", "C", "C", "C", "Cl"], "Bonds": "...", "Coordinates": "..."}]}
```

[Tool: Graph2SMILES]

Tool output:

```
{"reactants": "[Ar]C([R])=O", "products": "[Ar]C1([R])O[C@H](c2ccccc2Cl)N(S(=O)(=O)c2ccc(C)cc2)C1=O"}
```

Final output

Reaction Template SMILES: {"reactants": "[Ar]C([R])=O", "products": "[Ar]C1([R])O[C@H](c2ccccc2Cl)N(S(=O)(=O)c2ccc(C)cc2)C1=O"}

Fig. S4. Example workflow of Reaction template parsing agent. The agent extracts the reaction template by first using RxnImgParser to locate reactant and product regions, then Image2Graph to convert each region into an atom-bond graph. It detects the in-figure R-group definition, replaces the placeholder in the graph, and finally calls Graph2SMILES to output the complete SMILES template.

Prompt: You are the molecular recognition agent, your task is to detect and transfer every molecules in this reaction image into SMILES ...

Thought: I will check this image and call tools to recognize every molecules.
Actions: Check the image, first call *MolDetector*.

(,,, Run *MolDetector* tool)

Observation: All molecules have been extracted.

Thought: I need to run the *Image2Graph* tool to process each molecule.

Actions: Call *Image2Graph*.

(,,, Run *Image2Graph* tool)

Observation: There is still R-group formulas " $Ar1 = 3,5-(CF3)2C6H3$, $Ar2 = 2-CIC6H4$ " in the image. There is a obvious OCR error in the tool output: [\[iP1\]](#)

Thought: I need to replace the R-group placeholders with the R-group formulas in the graph atom set, correct the OCR error, then run the *Graph2SMILES* tool.

Actions: Replace the R-group placeholders and correct the OCR errors.

Then Call *Graph2SMILES*.

(,,, Run *Graph2SMILES* tool)

Observation: The molecular SMILES are all correct but still no type and label.
Actions: Identify the type of each molecule and assign a label, then output the

Finally, the type of each molecule and its SMILES, are output in the final molecular SMILES list for further processing.

Molecular SMILES List

'[A][R]C1([R])O[C@H](c2cccccc2C)N(S(=O)(=O)c2ccc(C)cc2)C1=O: [3', 'reactant template'],
'[A][R]C1([R])O[C@H](c2cccccc2C)N(S(=O)(=O)c2ccc(C)cc2)C1=O: [3', 'product template'],
'CC[C@]1(c2cccccc2)O[C@H](c2cccccc2C)N(S(=O)(=O)c2ccc(C)cc2)C1=O: [3a', 'product'], **"1"**
'CCC[C@]1(c2cccccc2)O[C@H](c2cccccc2C)N(S(=O)(=O)c2ccc(C)cc2)C1=O: [3b', 'product'],

CCCC(C=C=C)C1=C1[N+2]=CN3[\square @H](C1=C(CC=C1C(F)(F))C(F)(F))(C1=CC(=CC(=C1C(F)(F))C(F)(F))O)CCC3=N2.F[B-J](F)F': ['B17', 'conditions'], 'CCCC(C=C=C)C1=C1[N+2]=CN3[\square @H](C1=C(CC=C1C(F)(F))C(F)(F))(C1=CC(=CC(=C1C(F)(F))C(F)(F))O)CCC3=N2.F[B-J](F)F': ['B27', 'conditions'] "2"}

Fig. S5. Example workflow of Molecular recognition agent. The agent first calls MolDetector to locate every molecule in the reaction image, including both template and variant structures. It then invokes Image2Graph to convert each detected region into a detailed atom-bond graph. The agent identifies in-figure R-group definitions and corrects OCR errors (for example changing “iP1” to “iPr”), updates the corresponding atom sets, and finally uses Graph2SMILES to generate fully resolved SMILES strings for each molecule, ready for downstream processing.

Prompt: You are the structure-based R-group substitution agent, you will receive the output from reaction template parsing agent and molecular recognition agent, your task is to call tools to reconstruct complete reaction SMILES ...

Thought: I will check the output from reaction template parsing agent and molecular recognition agent and call tools to reconstruct complete reaction SMILES using these output.

Actions: Check the output, Then call SMILESReconstructor.

(,, Run SMILESReconstructor tool)

Observation: All detailed reactions have been reconstructed and are correct.
Actions: Output the complete Reaction SMILES List.

[Tool: SMILESReconstructor]

Tool input 1: Output from reaction template parsing agent

Tool input 2: Output from molecular recognition agent

Tool output:

```
{"reactions": {"3a": {"reactants": "[CCC(=O)c1ccccc1]", "products": "[CC[C@]1(c2cccc2)O[C@H](c2cccc2Cl)N(S(=O)(=O)c2ccc(C)cc2)C1=O"]}, "3b": {"reactants": "[CCCC(=O)c1ccccc1]", "products": "[CC[C@]1(c2cccc2)O[C@H](c2cccc2Cl)N(S(=O)(=O)c2ccc(C)cc2)C1=O"]}, "3c": {...}},
```

Reaction SMILES List:

```
{"reaction_template": {"reactants": "[[Ar]C([R])=O]", "products": "[[Ar]C1([R])O[C@H](c2cccc2Cl)N(S(=O)(=O)c2ccc(C)cc2)C1=O"]}, "reactions": {"3a": {"reactants": "[CCC(=O)c1ccccc1]", "products": "[CC[C@]1(c2cccc2)O[C@H](c2cccc2Cl)N(S(=O)(=O)c2ccc(C)cc2)C1=O"]}, "3b": {"reactants": "[CCCC(=O)c1ccccc1]", "products": "[CC[C@]1(c2cccc2)O[C@H](c2cccc2Cl)N(S(=O)(=O)c2ccc(C)cc2)C1=O"]}, "3c": ...}, "3c": ...}, "CCCC(C=CC=C1)=C1[N+]=CN3[C@H](C(C1=CC(=CC(=C1C(F)(F)C(F)(F)F))(C1=CC(=CC(=C1C(F)(F)C(F)(F)F))(C1=CC(=C1C(F)(F)C(F)(F)F))O)CCC3=N2.F[B-](F)F": [B17, "conditions"], "CCCC(C=CC=C1)=C1[N+]=CN3[C@H](C(C1=CC(=CC(=C1C(F)(F)C(F)(F)F))(C1=CC(=C1C(F)(F)C(F)(F)F))O)CCC3=N2.F[B-](F)F": [B27, "conditions"]}}
```

Final output

Fig. S6. Example workflow of Structure-based R-group substitution agent. The agent uses outputs from the Reaction Template Parsing and Molecular Recognition agents to rebuild full reactant SMILES for each reaction variant. It invokes SMILESReconstructor to align each product variant structure's R-group fragment with the product template, extract the correct substituent strings, and splice them into the reactant scaffold, yielding fully resolved reactant-variant SMILES ready for downstream integration and tasks.

Prompt: You are the text-based R-group substitution agent, you will receive the output from reaction template parsing agent, your task is to parse the table in this reaction image, replace the R-group placeholders in the reaction template with the detailed R-groups in the table row by row, then call tools to reconstruct complete reaction SMILES ...

Thought: I will check the output from reaction template parsing agent, replace the R-group placeholders in the reaction template with the detailed R-groups in the table row by row, then call tools to reconstruct complete reaction SMILES .

Actions: Check the output, First call *TableParser*.

(,,, Run *TableParser* tool)

Observation: All detailed R-groups in the table have been extracted.

Thought: I need to replace the R-group placeholders in the graph atom set in reaction template with the detailed R-groups in the table row by row, then call tools to reconstruct complete reaction SMILES.

Actions: Replace the R-group placeholders row by row:

```
>{"C", "[R1]", "C", "C", "[R2]", "O", "C", "[CN]", "C", "[R3]", "O", "C", "[R4]"],  
{"C", "[R4]", "C", "[CN]", "C", "[R3]", "O", "C", "[R1]", "C", "C", "O", "C", "[R2]"} →  
{"C", "[Ph]", "C", "C", "[H]", "O", "C", "[CN]", "C", "[Ph]", "O", "C", "[4-BrC6H4]"},  
{"C", "[4-BrC6H4]", "C", "[CN]", "C", "[Ph]", "O", "C", "[Ph]", "C", "O", "C", "[H]"};  
{"C", "[Ph]", "C", "C", "[H]", "O", "C", "[CN]", "C", "[Ph]", "O", "C", "[3-BrC6H4]"},  
{"C", "[3-BrC6H4]", "C", "[CN]", "C", "[Ph]", "O", "C", "[Ph]", "C", "C", "O", "C", "[H]"} ...  
Then call Graph2SMILES.
```

(,,, Run *Graph2SMILES* tool)

Observation: All detailed reactions have been reconstructed and are correct.

Actions: Output the complete Reaction SMILES List.

[**Tool: TableParser**]

Tool output:

```
[{"entry":1,"R1":"Ph","R2":"H","R3":"Ph","R4":"4-BrC6H4","time":24,"product":"3a","yield":78},  
{"entry":2,"R1":"Ph","R2":"H","R3":"Ph","R4":"3-BrC6H4","time":24,"product":"3b","yield":67},  
{"entry":3,"R1":"Ph","R2":"H","R3":"Ph","R4":"2-BrC6H4","time":24,"product":"3c","yield":78}, ... ]
```

[**Tool: Graph2SMILES**]

Tool output:

```
{"reactions":{"3a":{"reactants":["[H]CC(=O)C#Cc1cccc1","N#CC=Cc1ccc(Br)cc1C(=O)c1cccc1"],"products":["[H]C1C(=O)/C=C(c2cccc2)O/C(c2cccc2)=C(/C#N)C1c1cc(Br)cc1"]},  
"3b":{"reactants":["[H]CC(=O)C#Cc1cccc1","N#CC=Cc1ccc(Br)cc1C(=O)c1cccc1"],"products":["[H]C1C(=O)/C=C(c2cccc2)O/C(c2cccc2)=C(/C#N)C1c1cccc(Br)c1"]},  
"3c":{"reactants":["[H]CC(=O)C#Cc1cccc1","N#CC=Cc1cccc1Br)C(=O)c1cccc1"],"products":["[H]C1C(=O)/C=C(c2cccc2)O/C(c2cccc2)=C(/C#N)C1c1cccc1Br"]}}}
```

Final output

Reaction SMILES List:

```
{'reaction_template': {'reactants': '[R1]C#CC(=O)C[R2]', '[R3]C(=O)/C(C#N)=C/[R4]'},  
'products': '[R1]/C1=C/C(=O)C([R2])/C([R4])/C(C#N)=C(/[R3])O1'},  
"reactions": {"3a": {"reactants": "[H]CC(=O)C#Cc1cccc1", "N#CC=Cc1ccc(Br)cc1C(=O)c1cccc1"}, "products": "[H]C1C(=O)/C=C(c2cccc2)O/C(c2cccc2)=C(/C#N)C1c1cccc(Br)cc1"},  
"3b": {"reactants": "[H]CC(=O)C#Cc1cccc1", "N#CC=Cc1cccc(Br)c1C(=O)c1cccc1"}, "products": "[H]C1C(=O)/C=C(c2cccc2)O/C(c2cccc2)=C(/C#N)C1c1cccc(Br)c1"},  
"3c": {"reactants": "[H]CC(=O)C#Cc1cccc1", "N#CC=Cc1cccc1Br)C(=O)c1cccc1"}, "products": "[H]C1C(=O)/C=C(c2cccc2)O/C(c2cccc2)=C(/C#N)C1c1cccc1Br"]}, ... }
```

Fig. S7. Example workflow of Text-based R-group substitution agent. The agent first invokes *TableParser* to harvest R-group definitions row by row from an accompanying text table, then replaces each placeholder in the reactant and product graphs with the extracted substituents. Finally, it calls *Graph2SMILES* to emit fully resolved SMILES for every reaction variant, seamlessly rebuilding all reactant-product combinations.

Prompt: You are the condition interpretation agent, your task is to extract the reaction condition texts in this reaction image, interpret the condition texts then output full condition list

Thought: I will check this image and call tools to output full condition list.
Actions: Check the image, first call *TesseractOCR*.

(,,, Run *TesseractOCR* tool)

Observation: All reaction condition texts have been extracted.

Thought: I need to run the *RxnConInterpreter* tool to interpret all the condition texts by identifying their condition roles.

Actions: Call *RxnConInterpreter*.

(..., Run *RxnConInterpreter* tool)

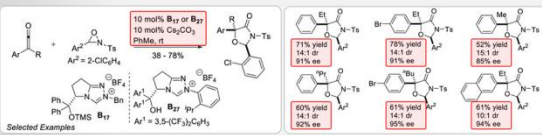
Observation: All reaction condition texts have been extracted, interpreted

and the results are correct, but haven't align with the Reaction SMILES List.

Actions: Align the interpreted reading with the original text.

[Tool: *TesseractOCR*]

Tool output



```

Reaction Condition List:
{ "reaction_template": { "conditions": { "role": "reagent", "text": "10 mol% B17 or B27", "smiles": "C(C=CC=C1)=C1C[N+]2=CN3[C@H](C(C4=CC=CC=C4)(C5=CC=CC=C5)O[Sij](C)C(C)(C)C)CCC3=N2.F[B-](F)(F)F", "label": "B17"}, { "role": "reagent", "text": "10 mol% B17 or B27", "smiles": "CCCC(C=CC=C1)=C1[N+]2=CN3[C@H](C(C1=CC(=CC(=C1C(F)(F)F)C(F)(F)F)(C1=CC(=CC(=C1C(F)(F)F)C(F)(F)F)O)CCC3=N2.F[B-](F)(F)F", "label": "B27"}, { "role": "reagent", "text": "10 mol% Cs2CO3", "smiles": "[Cs+].[Cs+].[O-]C(=O)[O-]", "label": "Cs2CO3"}, { "role": "solvent", "text": "PhMe", "smiles": "Cc1ccccc1"}, { "role": "temperature", "text": "rt"}, { "role": "yield", "text": "38 - 78%"}, "reactions": { "3a": { "conditions": { "role": "yield", "text": "71%"}, { "role": "add_info", "text": "14:1 dr"}, { "role": "add_info", "text": "91% ee"}, "label": "3a"}, "3b": { "conditions": { "role": "yield", "text": "78%"}, { "role": "add_info", "text": "14:1 dr"}, { "role": "add_info", "text": "91% ee"}, "label": "3b"}, "3c": { "conditions": { "role": "yield", "text": "78%"}, { "role": "add_info", "text": "14:1 dr"}, { "role": "add_info", "text": "91% ee"}, "label": "3c"} } }

```

Final output

Fig. S8. Example workflow of Condition interpretation agent. The agent first applies OCR tool to capture all textual annotations of reagents, solvents, temperatures, times and yields from the reaction image. It then invokes RxnConInterpreter to assign each text fragment to its proper condition role and align the output with the previously parsed reaction SMILES list.

Prompt: You are the text extraction agent, your task is to extract the text description in this reaction image, then extract the reactions and chemical identities in the text description...

Thought: I will check this image and call tools to extract the text description.
Actions: Check the image, first call *TesseractOCR*.

(,,, Run *TesseractOCR* tool)

Observation: The text description has been extracted.

Thought: I need to run the *MolNER* tool to extract the and chemical identities in the text description.

Actions: Call *MolNER*.

(,,, Run *MolNER* tool)

Observation: The chemical identities have been extracted.

Thought: I still need to run the *ChemRxnExtractor* tool to extract the reactions in the text description.

Actions: Call *ChemRxnExtractor*.

(,,, Run *ChemRxnExtractor* tool)

Observation: The chemical identities and the reactions have been extracted and the results are all correct. The detail of B27 have been extracted previously.
Actions: Output the final text extraction output with the detail of B27.

[Tool: *TesseractOCR*]

Tool output:

In 2010, an enantioselective formal cycloaddition of NHC-bound azolium enolates and oxaziridines was described by Ye and co-workers. Aryl(alkyl)-disubstituted ketenes were used as precursors of azolium enolates. A bifunctional NHC precatalyst B27 bearing a free hydroxyl group was employed.

[Tool: *MolNER*]

Tool output:

In 2010, an enantioselective formal [3+2] cycloaddition of NHC-bound azolium enolates [MULTIPLE] and oxaziridines [SYSTEMATIC] was described by Ye and co-workers. Aryl(alkyl)-disubstituted ketenes were used as precursors of azolium enolates. A bifunctional NHC [ABBREVIATION] precatalyst B27 [IDENTIFIERS] bearing a free hydroxyl group was employed.

[Tool: *ChemRxnExtractor*]

Tool output:

In 2010, an enantioselective formal [3+2] cycloaddition of NHC-bound azolium enolates [reactant] and oxaziridines [reactant] was described by Ye and co-workers. Aryl(alkyl)-disubstituted ketenes were used as precursors of azolium enolates [reactant]. A bifunctional NHC [ABBREVIATION] precatalyst B27 [reagent] [IDENTIFIERS] [SMILES:CCCC(C=CC=C1)=C1[N+](=O)[O-]2=CN3[C@H](C(C1=CC(=CC=C1C(F)(F)C(F)(F)C(F)(F))C1=CC(=CC=C1C(F)(F)C(F)(F)C(F)(F))O)CCC3=N2.F[B-](F)(F)F] bearing a free hydroxyl group was employed.

Final output

Text Extraction Output: {"In 2010, an enantioselective formal [3+2] cycloaddition of **NHC-bound azolium enolates [reactant]** [**MULTIPLE**] and **oxaziridines [reactant]** [**SYSTEMATIC**] was described by Ye and co-workers. Aryl(alkyl)-disubstituted ketenes were used as precursors of **azolium enolates [reactant]**. A bifunctional NHC [**ABBREVIATION**] precatalyst **B27 [reagent]** [**IDENTIFIERS**] [**SMILES:CCCC(C=CC=C1)=C1[N+](=O)[O-]2=CN3[C@H](C(C1=CC(=CC=C1C(F)(F)C(F)(F)C(F)(F)C(F)(F))C1=CC(=CC=C1C(F)(F)C(F)(F)C(F)(F))O)CCC3=N2.F[B-](F)(F)F**] bearing a free hydroxyl group was employed."}

Fig. S9. Example workflow of Text extraction agent. The agent first runs *TesseractOCR* tool to capture all text. Next, it uses *MolNER* to label each chemical name according to its class. Finally, it calls *ChemRxnExtractor* to assign reaction roles. The agent then links these extracted details back to earlier agent outputs; for example, the mention “B27” in the text is matched to the same reagent molecular structure parsed from the reaction template image. This reconciliation brings together text-derived information with image- and table-based data to form a unified, structured reaction record.

Supplementary Tables

Base	Model	Tani@1.0 (Abbreviation)	Tani@1.0 (Chiral)
Specialized	OpenChemIE	17.3	11.5
	MERMAid	6.1	5.5
Generalized	InterVL-V1.5	0.0	0.0
	Llama-3.2-Vision	0.0	0.0
Generalized	Qwen2.5-Max	1.1	0.5
	GPT-4o	3.2	2.0
	ChemEAGLE	80.2	75.4

Table S1. Tani@1.0 accuracy (in %) for molecules with abbreviations and chiral centers on the benchmark of multimodal chemical reaction graphics.

Base	Model	Valid SMILES Rate		
		Precision	Recall	F1
Specialized	DECIMER	74.1	22.4	34.4
	MolScribe	96.5	33.6	49.8
	MolNexTR	96.8	34.9	51.3
Generalized	InterVL-V1.5	6.7	3.5	4.6
	Llama-3.2-Vision	7.7	4.0	5.3
	Qwen2.5-Max	21.2	17.6	19.2
	GPT-4o	54.5	49.3	51.8
	ChemEAGLE	97.7	96.2	96.9

Table S2. Valid SMILES rate (in %) for molecular image recognition task on MultiMol dataset.

Base	Model	Avg Sim.	Tani@1.0
Specialized	DECIMER	15.1	11.7
	MolScribe	36.3	25.5
	MolNexTR	40.1	28.1
Generalized	InterVL-V1.5	5.2	4.4
	Llama-3.2-Vision	8.8	7.0
	Qwen2.5-Max	13.9	12.1
	GPT-4o	23.1	19.5
	ChemEAGLE	95.1	80.4

Table S3. Tanimoto similarity (Avg Sim., in %) and Tani@1.0 (in %) for molecular image recognition task on MultiMol dataset.

Base	Model	Valid SMILES Rate		
		Precision	Recall	F1
Specialized	RxndataExtractor	7.6	4.1	5.3
	RxnScribe	71.2	70.3	70.8
	RxnIM	73.4	72.6	73.0
Generalized	InterVL-V1.5	3.7	3.0	3.31
	Llama-3.2-Vision	7.0	5.3	6.03
	Qwen2.5-Max	12.1	10.9	11.5
	GPT-4o	17.3	14.7	15.9
	ChemEAGLE	76.3	74.2	75.2

Table S4. Valid SMILES rate (in %) for reaction image parsing task on ACS dataset.

Base	Model	Avg Sim.	Tani@1.0
Specialized	RxndataExtractor	3.2	1.3
	RxnScribe	66.2	61.2
	RxnIM	67.9	64.7
Generalized	InterVL-V1.5	3.0	2.9
	Llama-3.2-Vision	5.1	4.6
	Qwen2.5-Max	10.0	7.8
	GPT-4o	13.1	11.3
	ChemEAGLE	72.4	66.5

Table S5. Tanimoto similarity (Avg Sim., in %) and Tani@1.0 (in %) for reaction image parsing task on ACS dataset.

References

1. K. He, X. Zhang, S. Ren, J. Sun, Deep Residual Learning for Image Recognition. arXiv arXiv:1512.03385 [Preprint] (2015). <https://doi.org/10.48550/arXiv.1512.03385>.
2. A. Vaswani, N. Shazeer, N. Parmar, J. Uszkoreit, L. Jones, A. N. Gomez, L. Kaiser, Polosukhin, Attention Is All You Need. <https://arxiv.org/abs/1706.03762v7>.
3. T. Chen, S. Saxena, L. Li, D. J. Fleet, G. Hinton, Pix2seq: A language modeling framework for object detection. arXiv preprint arXiv:2109.10852 (2021).
4. J. Lee, W. Yoon, S. Kim, D. Kim, S. Kim, C. H. So, J. Kang, BioBERT: a pre-trained biomedical language representation model for biomedical text mining. *Bioinformatics* 36, 1234–1240 (2020).
5. J. Guo, A. S. Ibanez-Lopez, H. Gao, V. Quach, C. W. Coley, K. F. Jensen, R. Barzilay, Automated chemical reaction extraction from scientific literature. *Journal of chemical information and modeling* 62, 2035–2045 (2021).
6. Y. Chen, C. T. Leung, Y. Huang, J. Sun, H. Chen, H. Gao, MolNexTR: a generalized deep learning model for molecular image recognition. *Journal of Cheminformatics* 16, 141 (2024).
7. Z. Liu, H. Mao, C.-Y. Wu, C. Feichtenhofer, T. Darrell, S. Xie, “A ConvNet for the 2020s” in A Convnet for the 2020s. (2022), pp. 11976–11986.
8. A. Dosovitskiy, L. Beyer, A. Kolesnikov, D. Weissenborn, X. Zhai, T. Unterthiner, M. Dehghani, M. Minderer, G. Heigold, S. Gelly, J. Uszkoreit, N. Houlsby, An Image is Worth 16x16 Words: Transformers for Image Recognition at Scale. arXiv arXiv:2010.11929 [Preprint] (2021). <https://doi.org/10.48550/arXiv.2010.11929>.
9. J. Devlin, M.-W. Chang, K. Lee, K. Toutanova, Bert: Pre-training of deep bidirectional transformers for language understanding. arXiv preprint arXiv:1810.04805 (2018).
10. X. Zhu, W. Su, L. Lu, B. Li, X. Wang, J. Dai, Deformable DETR: Deformable Transformers for End-to-End Object Detection. arXiv arXiv:2010.04159 [Preprint] (2021). <https://doi.org/10.48550/arXiv.2010.04159>.
11. H. Touvron, L. Martin, K. Stone, P. Albert, A. Almahairi, Y. Babaei, N. Bashlykov, S. Batra, P. Bhargava, S. Bhosale, D. Bikel, L. Blecher, C. C. Ferrer, M. Chen, G. Cucurull, D. Esiobu, J. Fernandes, J. Fu, W. Fu, B. Fuller, C. Gao, V. Goswami, N. Goyal, A. Hartshorn, S. Hosseini, R. Hou, H. Inan, M. Kardas, V. Kerkez, M. Khabsa, I. Kloumann, A. Korenev, P. S. Koura, M.-A. Lachaux, T. Lavril, J. Lee, D. Liskovich, Y. Lu, Y. Mao, X. Martinet, T. Mihaylov, P. Mishra, I. Molybog, Y. Nie, A. Poulton, J. Reizenstein, R. Rungta, K. Saladi, A. Schelten, R. Silva, E. M. Smith, R. Subramanian, X. E. Tan, B. Tang, R. Taylor, A. Williams, J. X. Kuan, P. Xu, Z. Yan, I. Zarov, Y. Zhang, A. Fan, M. Kambadur, S. Narang, A. Rodriguez, R. Stojnic, S. Edunov, T. Scialom, Llama 2: Open Foundation and Fine-Tuned Chat Models. arXiv arXiv:2307.09288 [Preprint] (2023). <https://doi.org/10.48550/arXiv.2307.09288>.

12. J. Achiam, S. Adler, S. Agarwal, L. Ahmad, I. Akkaya, F. L. Aleman, D. Almeida, J. Altenschmidt, S. Altman, S. Anadkat, others, Gpt-4 technical report. arXiv preprint arXiv:2303.08774 (2023).